Journal of Nuclear Medicine, published on August 18, 2022 as doi:10.2967/jnumed.122.263962

Cure of Micrometastatic B-cell Lymphoma in a scid Mouse Model using ^{213}Bi Anti-CD20 Monoclonal Antibody

Gregory T. Havlena[+], Nirav S. Kapadia[+], Peng Huang , Hong Song,
James Engles, Martin Brechbiel , George Sgouros,
Richard L Wahl

[+]GK and NK contributed equally

*For correspondence :

Richard L. Wahl, M.D.
Mallinckrodt Institute of Radiology
Washington University in St Louis School of Medicine
510 S. Kingshighway Blvd
St. Louis, MO 63110

Financial Support: P50CA096888

Disclosure: No conflicts of interest

Word Count:

Running Title: ^{213}Bi Anti-CD20 Cures Human Lymphoma in Mice

---

Abstract:

Objectives We studied the feasibility of alpha emitter, ^{213}Bi -Anti-CD20 therapy with direct bioluminescent tracking of micrometastatic human B-cell Lymphoma in a scid Mouse Model.

Methods A highly-lethal SCID mouse model of minimal tumor burden disseminated NHL was established using human Raji lymphoma cells transfected to express the luciferase reporter. . *In vitro* and *in vivo* radioimmunotherapy experiments were conducted. Single and multiple dose regimens were explored and results with ^{213}Bi Rituximab compared to various controls including no treatment, free ^{213}Bi radiometal, unlabeled Rituximab, and ^{213}Bi-labeled anti-HER2/neu (non-CD20 specific antibody). ^{213}Bi Rituximab was also compared to the low energy beta-emitter ^{131}I I-Tositumomab and the high energy beta emitting ^{90}Y - Rituximab *in vivo*.

Results *In vitro* studies showed dose-dependent target-specific killing of lymphoma cells with ^{213}Bi Rituximab. Multiple *in vivo* studies showed significant and specific tumor growth delays with ^{213}Bi rituximab vs free ^{213}Bi, ^{213}Bi control antibody and rituximab. Re-dosing of ^{213}Bi rituximab was more effective than single dosing. With a single dose of therapy given at 4 days post iv tumor inoculation, all untreated controls and all mice in the 25µCi ^{90}Y -Rituximab group progressed. With 100µCi ^{213}Bi –Rituximab, 75% of the mice survived and all but one survivor was cured. With 55µCi ^{131}I I-Tositumomab, 75% of the mice were tumor free by BLI and 62.5% survived.

Conclusions Cure of micrometastatic NHL is achieved in the majority of animals treated at 4 days post-i.v tumor inoculation using either ^{213}Bi rituximab or ^{131}I tositumomab in contrast to the lack of cures with unlabeled rituximab, ^{90}Y rituximab or if there was high tumor burden before RIT. Alpha emitter labeled anti CD-20 antibodies are promising therapeutics for NHL although a longer lived alpha emitter may be of greater efficacy.

BACKGROUND:

Interest in radioimmunotherapy (RIT) began last century, but heightened with the FDA approval in 2002/3 of the anti CD20 radioimmunotherapies Zevalin (^{90}Y Ibritumomab tiuxetan) and Bexxar (Tositumomab and ^{131}I Tositumomab). They represent the only FDA-approved radioimmunotherapy agents (1), though ^{131}I tositumomab is no longer marketed in the US and Zevalin utilization is limited (2).

The FDA-approved radionuclides for anti CD20 radioimmunotherapy emit β-particles which differ from α-particle or Auger-electron radiation(3, 4). β-particles deposit energy along a relatively large distance (path length) resulting in energy deposition per unit distance traveled (linear energy transfer or LET) that is relatively low. The β-particle emitted by ^{90}Y travels an average path length of 2.7mm with an average decay emission energy of 0.93 MeV, with an average energy transfer of (0.93 MeV/2.7 mm ≈ 0.34 kev/μm). The ^{131}I beta particle travels an average distance of 0.8mm as it deposits an average of 0.19 MeV(5).

While monoclonal antibodies are targeted to individual cancer cells, ^{90}Y and ^{131}I deposit much of their energy beyond the single tumor cell diameter. The long β-particle paths for ^{131}I and ^{90}Y are potentially advantageous if all the targeted tumor cells do not bind the antibody or if delivery of the antibody is heterogeneous in tumors, as it results in a more uniform radiation dose across the tumor. However, the rather long path length makes it more difficult for these agents to kill isolated single neoplastic cells or very small oligometastatic tumors, as much of the energy is deposited remotely from the tumor. Furthermore, the relatively long path lengths traveled by these decay particles can increase the likelihood of normal tissue toxicity (6). Alpha particles are helium nuclei which travel a shorter path length and deposit approximately 200-400 times more energy along their path distance. Notably, the α-particle emitted by ^{213}Po (the short-lived daughter species of ^{213}Bi) travels an average of only 0.08 mm and is strikingly more energetic than its β-particle emitting counterparts (8.35 MeV)(5). In the case of RIT, this translates into more frequent double-stranded DNA breaks(7) and an increased likelihood of caspase-mediated apoptosis (8). ^{213}Bi and other alpha emitters represent promising candidates for the *single* cell kill necessary to cure isolated cancer cells or very small

volumes of metastatic disease. There is now an FDA approved alpha emitting radiopharmaceutical for bone metastases, Ra223 dichloride (9) .

The experiments we conducted utilized a bioluminescent imaging (BLI) reporter system for real-time monitoring of treatment response affording a sensitive view of very low tumor burden *in vivo* tumor kill kinetics (10) (11).

We describe the synthesis and evaluation of the monoclonal anti-CD20 antibody, Rituximab, labeled with the alpha emitter ^{213}Bi ($t_{1/2}$ = 46mins). *In vitro* response to treatment was monitored with serial luminometry against appropriate controls, whereas the *in vivo* response was monitored via sequential optical imaging of disseminated Raji (non-Hodgkins) lymphoma cell tumor burden in SCID mice. ^{213}Bi rituximab has been used in vitro and has shown substantial anti-tumor activity. It also has been used for biodistribution studies in animal models of human NHL. There are preliminary data of the use of ^{213}Bi rituximab in the treatment of patients with NHL. However, evaluation has not been extensive as in vivo therapeutic, presumably in part because the short half-life of ^{213}Bi perhaps seems ill-matched to the relatively slow targeting of intact monoclonal antibodies to solid tumors(12) (13). ^{213}Bi has shown promise in pre-targeting settings to treat subcutaneous and disseminated NHL(12) . However, our evaluation focused on an iv delivered and widely disseminated tumor model where a ^{213}Bi labeled intact radioantibody might be expected to target to tumor far more rapidly than delivery of such a large intact antibody to a relatively less well-perfused subcutaneous tumor. We also performed studies comparing ^{213}Bi rituximab to the previously FDA-approved *^{131}I antiCD20 (Tositumomab) and ^{90}Y rituximab.*

MATERIALS AND METHODS:

Detailed methods appear in the supplemental materials. EB- positive human Raji lymphoma tumor cells were lentivirally transfected with reporter genes GFP and luciferase (14). Rituximab (human/mouse chimeric IgG monoclonal anti-CD20) was obtained from Genentech/Biogen Idec (San Francisco, CA) and murine anti-HER-2/*neu* antibody 7.16.4 was obtained from the Sgouros laboratory. Antibody integrity was

verified via SDS-PAGE . Raji cell surface expression of CD20 and antibody immunoreactivity were verified by a quantitative CD20 assay. ^{131}I-Tositumomab was obtained from the Johns Hopkins Outpatient Center.

Rituximab and anti-HER-2/*neu* were conjugated to SCN-CHX-A"-DTPA as previously described (15, 16). The average number of chelates per antibody was approximately 1.6 (17). Immunoreactivity was determined by the Lindmo method *(18)*.

^{225}Ac was purchased from Oak Ridge National Laboratory or Curative Technologies. ^{213}Bi was eluted from an ^{225}Ac generator *(19)*. "Rituximab or antibody 7.16.4" conjugated to the chelate were prepared. The reaction efficiency and purity of radioimmunoconjugates were determined with TLC . ^{90}Y-labeled Rituximab was similarly prepared.

Following the generation of standard curves for Raji-GFP-Luc cell bioluminescence, 5 x 10^4 cells were measured on a Monolight 3010 Luminometer. Samples were divided into four groups: untreated controls, free radionuclide, and ^{213}Bi radiolabeled anti-CD20 (either blocked or unblocked with unlabeled anti-CD20). Antigenic blockade was accomplished with a 24-hour pre-dose of unlabeled anti-CD20 at a concentration of 50μg/ml. Serial counts were obtained daily for seven days or until no viable cells remained in culture in quadruplicate experiments.

CB57 (CB17) Balb/c scid mice (female) were intravenously injected with either 5.0 x 10^5 or 1.0 x 10^6 Raji-GFP-Luc lymphoma cells on day 0. Immediate *in vivo* bioluminescent imaging (BLI) confirmed successful intravenous tumor injection by the presence of quantifiable signal within the lungs. In the confirmed absence of tumor, mice were once again inoculated with intravenous tumor and re-imaged to confirm tumor dissemination.

In each of the four in vivo experiments, mice inoculated with tumor cells were treated with ^{213}Bi-Rituximab or one of several controls (Table 1). Single and multiple dose

regimens were explored and compared to no treatment, free ^{213}Bi radiometal, mass equivalent doses of unlabeled Rituximab, and ^{213}Bi-labeled anti-her2/neu (non-specific antibody). ^{213}Bi-Rituximab was also compared to anti CD-20 antibodies radiolabeled with beta-emitters, ^{131}I-Tositumomab and ^{90}Y- Rituximab. In all except one of the experiments treatments were initiated once exponential growth in tumor signal was established (14) to have taken place by day 7 post tumor inoculation. Treatment was initiated at an earlier time point (day 4) in a study comparing ^{213}Bi -labeled Rituximab to ^{131}I-Tositumomab or ^{90}Y-labeled Rituximab. . Radioactivity measurements were made in a Capintec dose calibrator (20).

Tumor burden was followed using the Xenogen IVIS® 200 Series Imaging System. every 2-7 days. Each animal served as its own reference, with results normalized to baseline pre-treatment tumor burdens obtained on day 4 or day (10). As tumor burden increased, the necessary acquisition time decreased . Optical images were analyzed via software provided by the manufacturer . Rectangular regions of interest were drawn around individual mice and average radiance [photons/(s)(cm^2)(sr)] was calculated by the software. This is also referred to as the relative light units per minute (RLU/min)) Mice were followed with intermittent optical imaging for 28, 131, 49, and 85 days respectively in *in vivo* experiments 1-4. In accordance with ethical guidelines, monitoring of a specific animal was discontinued in the event of a mouse death or any evidence of hind-leg paralysis (HLP) warranting euthanasia. In the first of four *in vivo* experiments animals were imaged for a preset period of four weeks, at which time all surviving animals in the study were sacrificed for pathologic analysis. In the remaining three studies intermittent imaging was continued until either all mice in a given study were experiment) or until all mice in the study with any evidence of tumor progression were deceased (experiments 2 and 4). In the latter category, mice without evidence of tumor progression were imaged for an additional several weeks following the final tumor-related death in the study to ensure they did not develop bioluminescent signal in excess of baseline as evidence of tumor progression. In all except experiment 1, overall survival was assessed by monitoring the mice, after the imaging period had ended, until death or

hind limb paralysis developed or when sacrifice of remaining animals was required for logistical reasons.

In each study the time from treatment until death (or hind limb paralysis), was assessed by Kaplan Meier analysis, ANOVA and t-tests. The RLU was monitored for each animal before and at multiple time points after therapy. A log transformation was applied to normalized RLU to analyze data from day 6 onward. A mixed effects model was fitted for each group separately to estimate its normalized RLU growth rate after day 6 (the baseline day). Calculations were performed using SAS.

Representative animals were identified for pathological assessment at the conclusion of experiment 1, when their disease had progressed sufficiently that humane sacrifice was required and when the studies were terminated with no evidence of tumor progression in experiments 2-4.

RESULTS:

The CHX-A'' DTPA conjugated antibodies were eluted from the reaction solution and concentrated to achieve final concentrations of approximately 10mg/ml, with an average of 1.6 chelators/antibody . After radiolabeling and purification 98.0+% purity was achieved. Lineweaver-Burke extrapolations generally determined the immunoreactive fraction to be at least 50% for the anti CD20 constructs.

Free ^{213}Bi at doses of >=10μCi/ml had dose-dependent anti-tumor effects in vitro ($p<0.05$). 2μCi/ml ^{213}Bi -Rituximab demonstrated selective cytotoxic effects ($p<0.01$) (figure 1). Specific cytotoxicity was absent (p=ns) with Rituximab blockade. Among unblocked samples, the number of cells doubled over a 6 day period while cells treated with the same dose after antigenic blockade multiplied 27-fold ($p<0.01$). At the 10μCi /ml dose of ^{213}Bi -Rituximab, net cytotoxicity (fewer cells than baseline) occurred within four days ($p<0.01$). This effect was blocked by rituximab ($p<0.01$). Complete cytotoxicity was observed at a 20μCi /ml dose with or without antigenic blockade

(p=0.48)(**Figure 1**). There was no difference in cell survival between the untreated controls and samples treated with 2μCi/ml of free ^{213}Bi but free ^{213}Bi an 10 and 20 uCi had anti-tumor effects (p=ns; supplemental **Figure 1).**

Table 1 summarizes the four in vivo experimental studies. Successful tumor injection was confirmed with immediate *in vivo* bioluminescent imaging. The absence of quantifiable signal above baseline, requiring repeat tumor injection, occurred in approximately 5% of injections. All groups of mice had quantifiable tumor bioluminescence detectable on the day of tumor inoculation. No differences in absolute tumor signal were found between any of the groups prior to the day of treatment in any of the four in vivo experiments. (n=NS). All groups had tumor growth above baseline on the last pre-treatment day. Initially intense lung cellular accumulation visible by BLI cleared quickly, so at two days following tumor administration, tumor burden was undetectable. Tumor was reliably detected sparsely throughout the animal at four days following injection. Three mice were found to have markedly increased tumor burden compared to the others ($p<0.01$) and were excluded from the therapeutic study as they developed macroscopic disease.

Overall survival duration was not assessed in Experiment 1 as animals were intentionally sacrificed at 28 days from tumor injection. After 28 days, all untreated mice in the died or developed HLP (requiring euthanasia) while in the groups treated with either a single dose of 35μCi or 100μCi of ^{213}Bi -Rituximab, all mice were alive without HLP. Two mice (40%) remained alive in the unlabeled Rituximab group, and three mice (60%) were alive in each of the other control groups (35μCi ^{213}Bi free radiometal and 35μCi ^{213}Bi-anti-HER2/*neu*) figure 2 and supplemental figure 2. Absolute Tumor burdens with the varying therapies are shown in supplemental Table 1.

In experiment 2 all untreated controls developed progressive tumor with HLP occurring from days 23-37 (figures 3a and 3b) . In the group treated with a single dose of 75μCi ^{213}Bi -Rituximab only 50% of the mice progressed and these died or developed HLP on days 33, 39, and 82. In the group treated with two doses 75μCi ^{213}Bi-Rituximab only 33% of the mice progressed developing HLP on days 45 and 72. 75% of mice

treated with two mass equivalent doses of unlabeled Rituximab progressed, developing HLP on days 57-79. All mice in the 75μCi ^{213}Bi -anti-HER2/*neu* group progressed and died or developed HLP from days 26-50.

In experiment 3 (figures 4 and supplemental figure 3) all untreated controls developed HLP from days 17-19. Animals treated with a single dose of 75 μCi ^{213}Bi-Rituximab developed HLP from days 26-32. Groups treated with two or three doses of 75μCi ^{213}Bi -Rituximab died or developed HLP from days 26-55 or days 31-42 respectively.

In experiment 4 (figures 5a-d and 6) all untreated controls developed HLP at days 20-40. In the group treated with a 100μCi ^{213}Bi -Rituximab only 25% of the mice progressed and these died or developed HLP on days 32 and 135. In the group treated with 55μCi ^{131}I-Tositumomab only 25% of the mice progressed and these died or developed HLP on days 38 and 155. 87.5% of mice treated with a mass equivalent dose of unlabeled Rituximab progressed and died or developed HLP from days 32-37 or from days on days 74-85. All mice in the 25μCi ^{90}Y-Rituximab group progressed and died or developed HLP from days 26-54.

Long-term remission/cure was defined as any animal without significant increase in tumor signal above the pre-treatment baseline on the final day of imaging in the three survival studies .

In experiment 2, (figures 3a and b) 1 of 4 (25%) of animals were cured in the treatment groups given two doses of 10μg unlabeled Rituximab, 2 of 6 (33%) of animals given a single dose of 75μCi ^{213}Bi -Rituximab, and 3 of 6 (50%) of animals given two doses of 75μCi ^{213}Bi -Rituximab met criteria for long-term remission/cure. In the latter two groups treated with one and two doses of the radiopharmaceutical one mouse in each group died secondary to complications from anesthesia during imaging on day 29. These mice were tumor free at the time of accidental death without significant bioluminescent signal above baseline. All mice in each of these groups that ultimately progressed to death secondary to tumor had already developed significant bioluminescent signals by day 29. The three mice that progressed to death secondary to tumor in the single dose

group had 13.6x, 1308x and 1508x the absolute bioluminescent signal, on day 29, of the mouse that died prematurely from anesthesia. In the two-dose group, the two mice that progressed had 51.7x and 60.5x the absolute bioluminescent signal of the mouse that died prematurely in that group. These two animals would likely have been counted among the cured in their respective groups except for their premature accidental deaths. Thus, a more accurate assessment of tumor cure rates could be 50% of the single dose of ^{213}Bi rituximab and 67% of the two doses of ^{213}Bi rituximab group. None of the mice in the untreated control group or group treated with two doses ^{213Bi}-anti-HER2/*neu* were cured.

No cures were achieved in experiment 3 (fig 4 and supplemental figure 3). In experiment 4 (figures 5 and 6 and supplemental figures 4 and 5), animals were cured in treatment groups given one dose of 10μg non-radioactive Rituximab, one dose of 100μCi ^{213}Bi -Rituximab, and one dose of 55μCi ^{131}I-Tositumomab. 1 of 8 (12.5%), 4 of 8 (50%), and 4 of 8 (50%) mice respectively met criteria for long-term remission/cure. None of the mice in the untreated control group or group treated with ^{90}Y-Rituximab were cured. Two mice in the ^{90}Y-Rituximab group died prematurely secondary to complications of anesthesia on day 12. Both mice had tumor progression beyond baseline comparable to the other mice in the same group and are unlikely to have been cured. Two mice in each of the ^{213}Bi -Rituximab and ^{131}I-Tositumomab groups died on days 58, 89 and days 18, 32 respectively without any increase in tumor signal above baseline. While these animals likely all represent additional cures, it is possible their premature death occurred as a result of treatment related toxicity. Thus, these animals were likely cured, so " cure" rates of 75% potentially can be claimed for both the 100μCi ^{213}Bi -Rituximab, and 55μCi ^{131}I-Tositumomab treated groups. It should be noted that BLI showed residual tumor in one animal each of the surviving 100μCi ^{213}Bi -Rituximab, and 55μCi ^{131}I-Tositumomab treated groups so these animals were not cured.

Linear mixed effects models were used compare rates of tumor progression among treatment groups. In order to assess tumor growth rates only among animals with actively growing tumor, animals that did not exhibit a significant increase in tumor signal above baseline pre-treatment levels (cured animals and animals without significant tumor progression at the time of death secondary to complications of anesthesia or treatment

related toxicity) were removed from each group prior to this analysis. In all four *in vivo* experiments the untreated control mice groups had significantly higher rates of tumor progression than all other treatment and control groups. In experiment 1 mice treated with a single dose of 35μCi ^{213}Bi Rituximab progressed slower than mice treated with either 35μCi free ^{213}Bi radiometal or 35μCi ^{213}Bi anti-HER2/*neu* (non-specific antibody) (figure 2 and supplemental table 1). In experiment 1, mice treated with a single dose of 100μCi ^{213}Bi -Rituximab progressed slower than those treated with a single dose of 35μCi ^{213}Bi Rituximab.

In experiment 2, mice treated with two doses of 75μCi ^{213}Bi -Rituximab progressed slower than mice treated with two doses of 75μCi ^{213}Bi-anti-HER2/*neu*. In experiment 2 (figures 3a, b) two doses 75μCi ^{213}Bi -Rituximab given on days 7 and 13 resulted slower tumor progression than one dose of 75μCi ^{213}Bi -Rituximab given on day 7, In Series 3 animals were inoculated with twice the initial dose of tumor as in Series 2. All animals (n=8 in each group) progressed and could be included in this analysis. In experiment 3, two or three doses of 75μCi ^{213}Bi -Rituximab given on days 7 and 12 or days 7, 12, and 19 respectively, significantly slowed tumor progression vs. single dose of 75μCi ^{213}Bi -Rituximab given on day 7 ($p < 0.0001$). The group treated with two doses had slower tumor progression than the group treated with three doses ($p=0.0229$). In experiment 4, detailed statistical analyses of changes in BLI and of survival are shown in supplemental tables 2-7 and supplemental figures 6,7,8a&b,9-11 (supplemental statistical data study 4) with BLI change findings consistent with survival data.

Adverse events related to these experiments involved mortality from the anesthetic procedure (n=6 distributed across all experiments). Histopathology was performed on multiple organs from representative animals across experiments. Untreated had a high tumor burden in multiple organs including the brain, marrow, kidney, liver, and mesentery. 35 uCi and 100uCi ^{213}Bi rituximab markedly reduced tumor burden. Mice treated with 35uCi or 100 uCi ^{213}Bi rituximab, had either no tumor cells in any organs or very limited residual tumor cells at a single site. Spleens from mice receiving 35μCi or 100μCi of ^{213}Bi rituximab were moderately contracted and had mild lymphoid

depletion. There was no other evidence of significant toxicity in any of the organs examined histologically, including kidneys.

DISCUSSION:

Our studies have demonstrated several important findings: ^{213}Bi rituximab could be reliably produced. . *In vitro* CD20-positive specific lymphoma cell killing was achieved . The i.v. tumor model system yielded disseminated NHL with a predictable pattern of lethality, including developing hind limb paralysis. ^{213}Bi rituximab was more effective at tumor cell kill in vitro and in vivo than free ^{213}Bi or ^{213}Bi anti-HER2/*neu* (non-specific antibody). A single dose of 100 uCi of ^{213}Bi rituximab given at 6 days post tumor injection was more active than 35 uCi ^{213}Bi rituximab or unlabeled rituximab. Dose response relationships were idetified.

While tumor growth delays could be achieved, animals with high tumor burdens at the start of therapy could not be reliably cured by ^{213}Bi rituximab, even with repeated dosing. For lower injected tumor cellular doses, including animals treated earlier in the course of their disease, cures were common particularly with ^{213}Bi rituximab. In experiment #4, where treatment was initiated at 4 days after 1 million cells were injected, one dose of 100μCi ^{213}Bi -Rituximab, and one dose of 55μCi ^{131}I-Tositumomab achieved cures in 4 of 8 (50%), and 4 of 8 (50%) mice respectively met criteria for long-term remission/cure, while two animals in each of the ^{213}Bi rituximab and ^{131}I-Tositumomab expired without detectable tumor, thus a 75% cure rate could be considered . None of the mice in the untreated control group or the group treated with ^{90}Y-Rituximab were cured.

Alpha emitters have previously been used to radiolabel anti CD-20 antibodies. Roscher et al showed activity of ^{213}Bi rituximab in vitro in chemosensitive and chemoresistant lymphoma cells. ^{213}Bi rituximab treatment appeared to restore caspase activity in vitro (21). Vandenbulke has shown an RBE of up to 5 for ^{213}Bi rituximab *in vitro* in killing

human CLL cells (13) . Intact ^{213}Bi rituximab was also active in vitro in our experiments where radioantibody access to tumor cells was nearly immediate, paralleling the antibody access to tumor cells in our in vivo model .

^{213}Bi -1F5 intact anti CD20 was evaluated for biodistribution to subcutaneous lymphoma xenografts by Park (12). At 45 minutes post injection, the Tumor/Blood uptake ratio was only .06 with 3% ID/g in tumor, equivalent to a non-specific antibody. Given this poor targeting to SQ tumor models, investigators did not perform therapy studies with the ^{213}Bi labeled intact anti CD20 , rather focusing on a pre-targeting approach (12).

We showed that the i.v. tumor model is treated successfully by the iv.^{213}BiRituximab, with cures possible in a many animals (series 4 experiments). Thus, intact antibodies which have very slow localization to SQ tumors have substantial therapeutic efficacy, even with 46 minute T ½ of ^{213}Bi, in the setting of disseminated lymphoma. Ostensibly, this finding defies the common wisdom regarding the suitable half-life for therapeutic isotopes used with intact monoclonal antibodies. Our data show the clear feasibility of intact radioantibody therapy with short lived alpha emitters in systems where intact antibodies reach tumor quickly. Schmidt et al have used ^{213}Bi anti CD20 antibodies to treat 12 patients with NH in an early phase study (22) .

^{211}At IF5 (anti CD20) slowed tumor growth in SQ lymphoma tumor xenografts, but did not achieve cures. However, an approximately 70% cure rate was seen with a solitary injection of ^{211}At IF5 at 2-6 days following an i.v. injection of 1 million tumor cells with stem cell support (23). Their cure rate is similar to ours using a single 75uCi dose of ^{213}Bi rituximab, but we did not use stem cell support. Alpha autoradiography of the subcutaneous tumors in the study by Green showed heterogeneous dose delivery, likely, accounting for the lack of cures in the subcutaneous (23). Higher tumor burdens in animal models are also associated with faster antibody clearance from the blood stream, potentially limiting treatment efficacy (24) . Alpha emitting ^{212}Pb (10.6 hr t ½) rituximab has demonstrated anti-tumor efficacy in B cell lymphoma model system in which 25,000

tumor cells were injected and treatment were initiated at 11 or more days post-injection(25).

^{227}Th (half-life of 18.7 days) rituximab was used to treat NHL xenografts (not MRD) with some cures(26, 27). ^{227}ThRituximab was superior in treatment efficacy *in vivo* to ^{90}Y ibritumomab tiuxetan and with a higher RBE (26). ^{227}Th decays to ^{223}Ra which can travel to normal bone , a potential limitation.

^{213}Bi rituximab, even with its very short half-life, has a significant therapeutic advantage over the first generation Y-90 anti CD20 therapy, in a disseminated MRD, model. Our data are intriguing as well, in that a high cure rate was seen when a single dose of ^{131}I tositumomab was used in the animal model with therapeutic efficacy comparable to ^{213}Bi rituximab. It appears the low energy ^{131}I beta emission, coupled with the 8 day half life of ^{131}I (to allow continued irradiation of tumors over days) , is a viable choice for eliminating minimal residual disease despite the limitation of the longer beta path length. These pre-clinical observations may help explain some of the very long clinical remissions reported using ^{131}I tositumomab (28) . We had a very limited supply of ^{131}I tositumomab, so it was not possible to systematically compare the beta emitting therapy to ^{213}Bi Rituximab in larger studies. It is unlikely the difference in the therapeutic effects was due to the differences in the underlying anti CD20 antibodies , rituximab a mouse/human chimera and tositumomab a purely murine reagent.

Our studies add to the emerging literature that a wide range of alpha emitters can be used to treat human malignancies *in vivo* in animal models and suggest considerable potential for *in vivo* translation. The short half life of ^{213}Bi of 46 minutes is a practical logistical limitation, but it allows for a very high dose rate if the alpha emitter binds quickly to the tumor. Longer -lived alpha emitters may be of greater potential. ^{225}Ac (10 day T1/2 may be ideally matched to the localization kinetics of intact rituximab or related antibodies without the ^{223}Ra daughter of ^{227Th}, though with a ^{213}Bi daughter which can circulate distantly.

It remains unclear why we were unable to achieve cures in all cases. A logical presumption is that the a larger tumor burden with more bulky disease limiting ^{213}Bi rituximab accessibility . This was not problematic when therapies were started earlier such as our fourth experiment with therapy given at 4 days post tumor cell injection. Our histology studies showed the emergence of bulky tumor which likely would not have had good access of the radioantibodies to the tumor in the time of the half-life of the ^{213}Bi rituximab treatment.

There are limitations to our study: Beta emitter labeled anti CD20 antibodies were limited to the final study and, ^{131}I tositumomab (a purely murine monoclonal) was compared to ^{90}Y and ^{213}Bi rituximab (a mouse-human chimeric antibody) . Thus, there could have been varying impacts of the antibody itself. While unlabeled rituximab has activity in our system, it is unlikely the excellent results with ^{131}I tositumomab are simply due to the murine antibody (3). It is also not totally clear that the maximum tolerated dose was given for each radioimmunotherapeutic agent, thus there is room for additional study.

Anti CD20 radioimmunotherapies have not been a great commercial success to date, but they are very active therapies, and there remain a variety of B cell lymphomas which remain incurable. The efficacy of the short-lived ^{213}Bi rituximab in curing disseminated NHL in animals lends support to the re-evaluation of anti CD20 radioimmunotherapy, with alpha emitter labeling, potentially using the longer lived ^{225}Ac.

Key Points:

QUESTION: Can ^{213} Bi anti-CD20 rituximab be produced and effectively treat micrometastatic human NHL in vitro and in an animal model?

PERTINENT FINDINGS: ^{213}Bi Rituximab showed specific lymphoma cytotoxicity *in vitro* and significant anti-lymphoma treatment efficacy *in vivo* vs free ^{213}Bi, ^{213}Bi control antibody, ^{90}Y rituximab and rituximab. In the group treated with a 100µCi ^{213}Bi – Rituximab or I-131 tositumomab 75% of the mice became tumor free with cures most common.

IMPLICATIONS FOR PATIENT CARE: ^{213}Bi rituximab is an active therapeutic for NHL although a longer-lived alpha emitter would likely be more effective.

REFERENCES:

1. Goldenberg D. Targeted Therapy of Cancer with Radiolabeled Antibodies. J Nucl Med. 2002;43(5):693-713.
2. Gleisner KS, Spezi E, Solny P, Gabina PM, Cicone F, Stokke C, et al. Variations in the practice of molecular radiotherapy and implementation of dosimetry: results from a European survey. EJNMMI physics. 2017;4(1):28.
3. Davis ea. The radioisotope contributes significantly to the activity of radioimmunotherapy. Clin Cancer Res. 2004;10:7792-8.
4. Knox SJ ea. Y-90 labeled anti-CD20 monoclonal antibody therapy of recurrent B-cell lymphoma. Clin Cancer Res. 1996;2:457-70.
5. Koppe MJ ea. Antibody-guided radiation therapy of cancer. Cancer and Met Rev. 2005;24:539-67.
6. Raylman RR, Clavo AC, Crawford SC, Recker B, Wahl RL. Magnetically-enhanced radionuclide therapy (MERiT): in vitro evaluation. International journal of radiation oncology, biology, physics. 1997;37(5):1201-6.
7. Claesson AK SB, Jacobsson L, Elmroth K. Relative biological effectiveness of the alpha-particle emitter (211)At for double-strand break induction in human fibroblasts. Radiation Research. 2007;167(3):312-8.
8. Friesen C GG, Koop B, Schwarz K, Morgenstern A, Apostolidis C, Debatin KM, Reske SN. Breaking chemoresistance and radioresistance with [213Bi]anti-CD45 antibodies in leukemia cells. Cancer Res. 2007;67(5):1950-8.
9. Parker C, Nilsson S, Heinrich D, Helle SI, O'sullivan J, Fosså SD, et al. Alpha emitter radium-223 and survival in metastatic prostate cancer. New England Journal of Medicine. 2013;369(3):213-23.
10. Klerk CP, Overmeer RM, Niers TM, Versteeg HH, Richel DJ, Buckle T, et al. Validity of bioluminescence measurements for noninvasive in vivo imaging of tumor load in small animals. Biotechniques. 2007;43(S1):S7-S13, S30.
11. Michel RB ea. Experimental therapy of disseminated B-cell lymphoma xenografts with 213-bismuth labeled anti-CD74. Nuclear Medicine and Biology. 2003;30:715-23.
12. Park SI, Shenoi J, Pagel JM, Hamlin DK, Wilbur DS, Orgun N, et al. Conventional and pretargeted radioimmunotherapy using bismuth-213 to target and treat non-Hodgkin lymphomas expressing CD20: a preclinical model toward optimal consolidation therapy to eradicate minimal residual disease. Blood. 2010;116(20):4231-9.
13. Vandenbulcke K, De Vos F, Offner F, Philippé J, Apostolidis C, Molinet R, et al. In vitro evaluation of 213Bi-rituximab versus external gamma irradiation for the treatment of B-CLL patients: relative biological efficacy with respect to apoptosis induction and chromosomal damage. Eur J Nucl Med Mol Imaging. 2003;30(10):1357-64.
14. Baba S CS, Ye Z, Cheng L, Engles JM, Wahl RL. How Reproducible is Bioluminescent Imaging of Tumor Cell Growth?: Single Time Point v.s. Dynamic Measurement Approach. Mol Imaging. 2007:In Press.
15. Nikula TK, McDevitt MR, Finn RD, Wu C, Kozak RW, Garmestani K, et al. Alpha-emitting bismuth cyclohexylbenzyl DTPA constructs of recombinant humanized anti-CD33 antibodies: pharmacokinetics, bioactivity, toxicity and chemistry. Journal of Nuclear Medicine. 1999;40:166-76.

16. Brechbiel MW, Gansow OA. Synthesis of C-functionalized trans-cyclohexyldiethylenetriaminepenta-acetic acids for labelling of monoclonal antibodies with the bismuth-212 α-particle emitter. Journal of the Chemical Society, Perkin Transactions 1. 1992(9):1173-8.
17. Pippin CG, Parker TA, McMurry TJ, Brechbiel MW. Spectrophotometric method for the determination of a bifunctional DTPA ligand in DTPA-monoclonal antibody conjugates. Bioconjugate chemistry. 1992;3(4):342-5.
18. Lindmo T, Boven E, Cuttitta F, Fedorko J, Bunn Jr P. Determination of the immunoreactive function of radiolabeled monoclonal antibodies by linear extrapolation to binding at infinite antigen excess. Journal of immunological methods. 1984;72(1):77-89.
19. McDevitt MR, Finn RD, Sgouros G, Ma D, Scheinberg DA. An 225Ac/213Bi generator system for therapeutic clinical applications: construction and operation. Applied Radiation and Isotopes. 1999;50(5):895-904.
20. Siegel JA, Zimmerman BE, Kodimer K, Dell MA, Simon WE. Accurate dose calibrator activity measurement of 90Y-ibritumomab tiuxetan. Journal of Nuclear Medicine. 2004;45(3):450-4.
21. Roscher M, Hormann I, Leib O, Marx S, Moreno J, Miltner E, et al. Targeted alpha-therapy using [Bi-213]anti-CD20 as novel treatment option for radio- and chemoresistant non-Hodgkin lymphoma cells. Oncotarget. 2013;4(2):218-30.
22. Schmidt D, Neumann F, Antke C, Apostolidis C, Martin S, Morgenstern A, et al. Phase 1 Clinical Study on Alpha-Therapy for Non-Hodgkin Lymphoma. Proceedings of the 4th Alpha-immunotherapy symposium. 2004:12.
23. Green DJ, Shadman M, Jones JC, Frayo SL, Kenoyer AL, Hylarides MD, et al. Astatine-211 conjugated to an anti-CD20 monoclonal antibody eradicates disseminated B-cell lymphoma in a mouse model. Blood. 2015;125(13):2111-9.
24. Daydé D, Ternant D, Ohresser M, Lerondel S, Pesnel S, Watier H, et al. Tumor burden influences exposure and response to rituximab: pharmacokinetic-pharmacodynamic modeling using a syngeneic bioluminescent murine model expressing human CD20. Blood. 2009;113(16):3765-72.
25. Durand-Panteix S, Monteil J, Sage M, Garot A, Clavel M, Saidi A, et al. Preclinical study of 212Pb alpha-radioimmunotherapy targeting CD20 in non-Hodgkin lymphoma. British journal of cancer. 2021;125(12):1657-65.
26. Dahle J, Borrebaek J, Jonasdottir TJ, Hjelmerud AK, Melhus KB, Bruland Ø S, et al. Targeted cancer therapy with a novel low-dose rate alpha-emitting radioimmunoconjugate. Blood. 2007;110(6):2049-56.
27. Dahle J, Krogh C, Melhus KB, Borrebaek J, Larsen RH, Kvinnsland Y. In vitro cytotoxicity of low-dose-rate radioimmunotherapy by the alpha-emitting radioimmunoconjugate Thorium-227-DOTA-rituximab. Int J Radiat Oncol Biol Phys. 2009;75(3):886-95.
28. Kaminski MS, Tuck M, Estes J, Kolstad A, Ross CW, Zasadny K, et al. 131I-tositumomab therapy as initial treatment for follicular lymphoma. New England Journal of Medicine. 2005;352(5):441-9.

Table 1: Summary of Mouse Experiments

Group Number	Treatment	Cells Injected	Number of "cures"
1	Untreated	1 x 10^6	0/5
1	^{213}Bi ritux 25 uCi (day 7)	1 x 10^6	0/5
1	^{213}Bi ritux 100 uCi (day 7)	1 x 10^6	0/5
1	^{213}Bi free 35 uCi (day 7)	1 x 10^6	0/5
1	^{213}Bi Her2/neu 35 uCi (day 7)	1 x 10^6	0/5
1	10 ug rituximab (day7)	1 x 10^6	0/5

Group Number	Treatment	Cells Injected	Number of "cures"
2	Untreated controls	5 x 10^5	0/6
2	^{213}Bi ritux 75 uCi (day 7)	5 x 10^5	2/6
2	^{213}Bi ritux 75 uCi (day 7,13)	5 x 10^5	3/7
2	10 ug rituximab (days 7,13)	5 x 10^5	1/4
2	^{213}Bi Her2/neu 75 uCi (day 7)	5 x 10^5	0/5

Group Number	Treatment	Cells Injected	Number of "cures"
3	Untreated controls	1 x 10^6	0/6
3	^{213}Bi ritux 75 uCi (day 7)	1 x 10^6	0/6
3	^{213}Bi ritux 75 uCi (days 7, 12)	1 x 10^6	0/6
3	^{213}Bi ritux 75 uCi (days 7,12,19)	1 x 10^6	0/6

Group Number	Treatment	Cells Injected	Number of "cures"
4	Untreated controls	1 x 10^6	0/8
4	^{213}Bi ritux 100 uCi (day 4)	1 x 10^6	6/8
4	^{131}I tositumomab 55 uCi (day 4)	1 x 10^6	6/8
4	^{Y90} rituximab 25 uCi (day 4)	1 x 10^6	0/8
4	10 ug rituximab (day4)	1 x 10^6	1/8

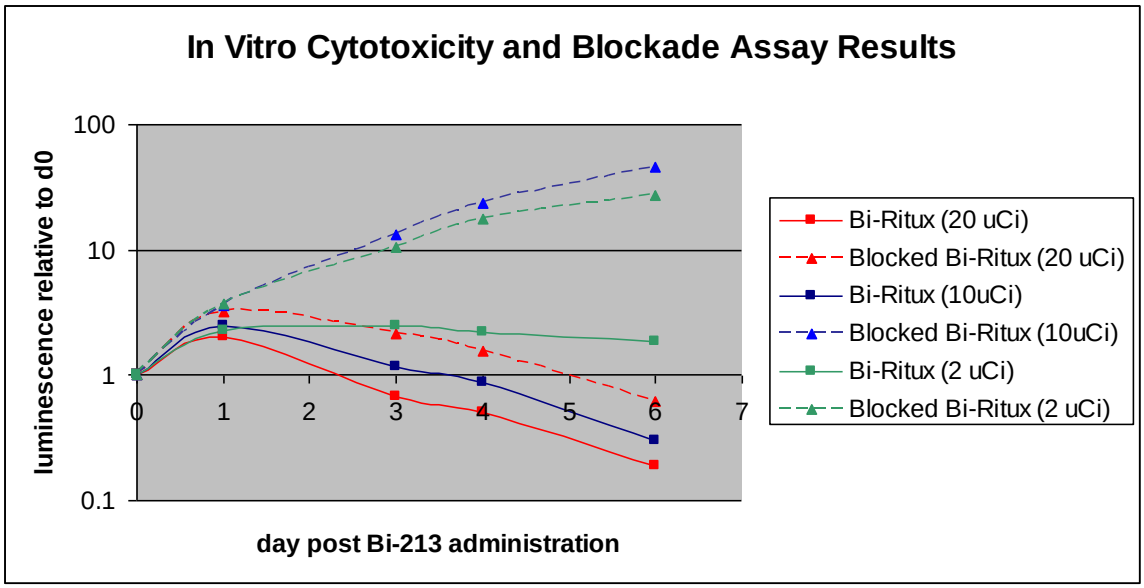

Figure 1: *In vitro* cytotoxicity by luminometry. Blockade was performed with 50 ug/ml of unlabeled rituximab for 24 hours prior to dosing with varying amounts of activity. Dose- dependent ^{213}Bi rituximab cell kill is substantially blocked with cold rituximab. X axis represents days of assessment (0-6 days). Controls (not shown) , blocked ^{213}Bi-Rituximab (2uCi and 10 uCi do not vary from one another over the 6 days, p=NS) . 2, 10 and 20 uCi of ^{213}Bi-Rituximab and 20 uCi of ^{213}Bi have significant anti-tumor effects vs the control and 2 and 10 uCi ^{213}Bi-Rituximab blocked groups ($p<.01$). ^{213}Bi-Rituximab and free ^{213}Bi at the 20 uCi doses were comparable (p=NS).

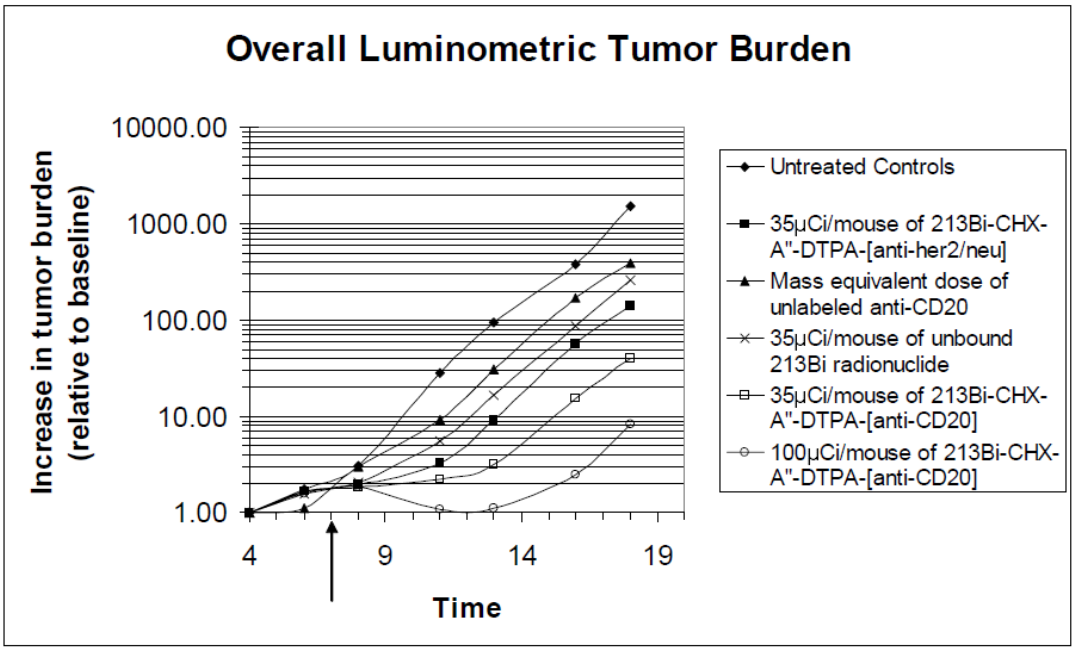

Figure 2: Experiment 1: In vivo tumor BLI growth curves are shown for the various treatment groups in experiment 1. The results are normalized to baseline tumor burdens obtained on day 4 (note log scale) . Time is measured from the point of intravenous tumor inoculation. Statistical significances between the various treatment and control arms at day 18 are displayed in supplemental table 1.

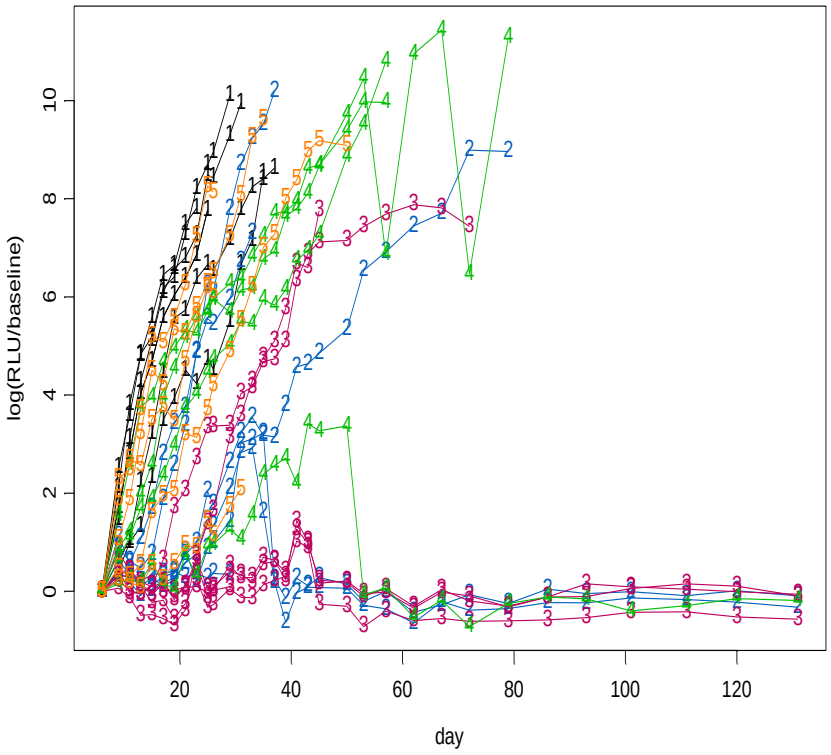

Figure 3a Experiment 2

Group

1 Controls
2 One Dose ^{213}Bi Rituximab (75uCi)
3 Two Doses ^{213}Bi Rituximab (75uCi x2)
4 Two Mass Equivalent Doses unlabeled Rituximab
5 Two Doses ^{213}Bi murine anti-HER-2/neu (antibody 7.16.4) (75uCi x2)

Individual animal RLU show two doses of ^{213}Bi Rituximab were the most effective..

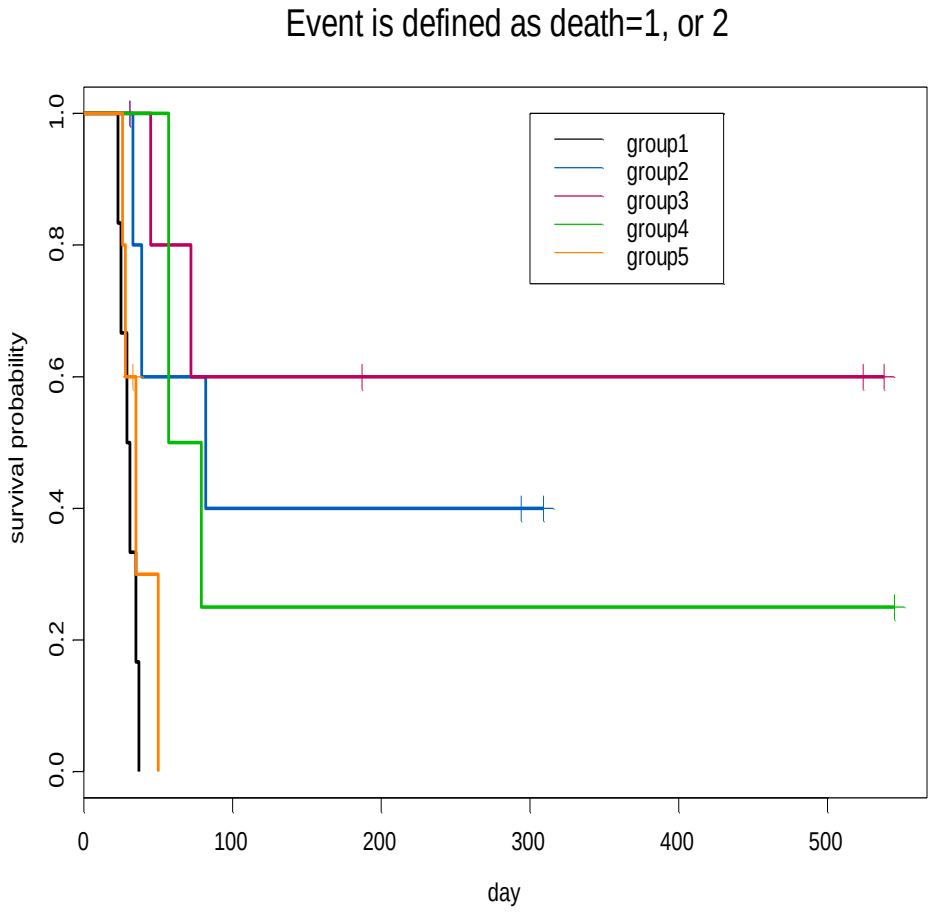

Figure 3b Experiment 2

Group	
1	Controls
2	One Dose 213Bi Rituximab (75uCi)
3	Two Doses 213Bi Rituximab (75uCi x2)
4	Two Mass Equivalent Doses unlabeled Rituximab
5	Two Doses 213Bi murine anti-HER-2/neu (antibody 7.16.4) (75uCi x2)

K-M plots show prolonged survival of the two dose and one dose of ^{213}Bi rituximab groups—groups 1 and 2.

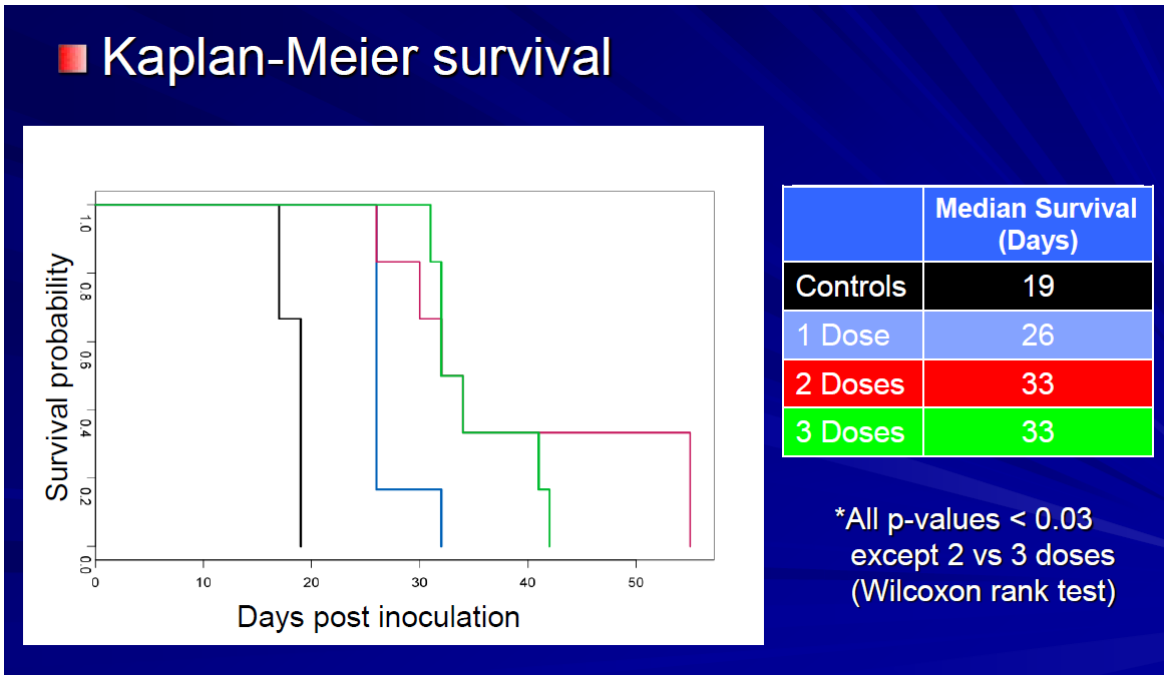

Figure 4: Experiment 3. There is a significant increase in median survival time with one dose of 213Bi rituximab relative to controls and with two/three doses relative to one dose. This study used a higher initial tumor inoculation with the same timing of first treatment as in Study 1. There were no cures in this study

Figures 5 a-d (panel)

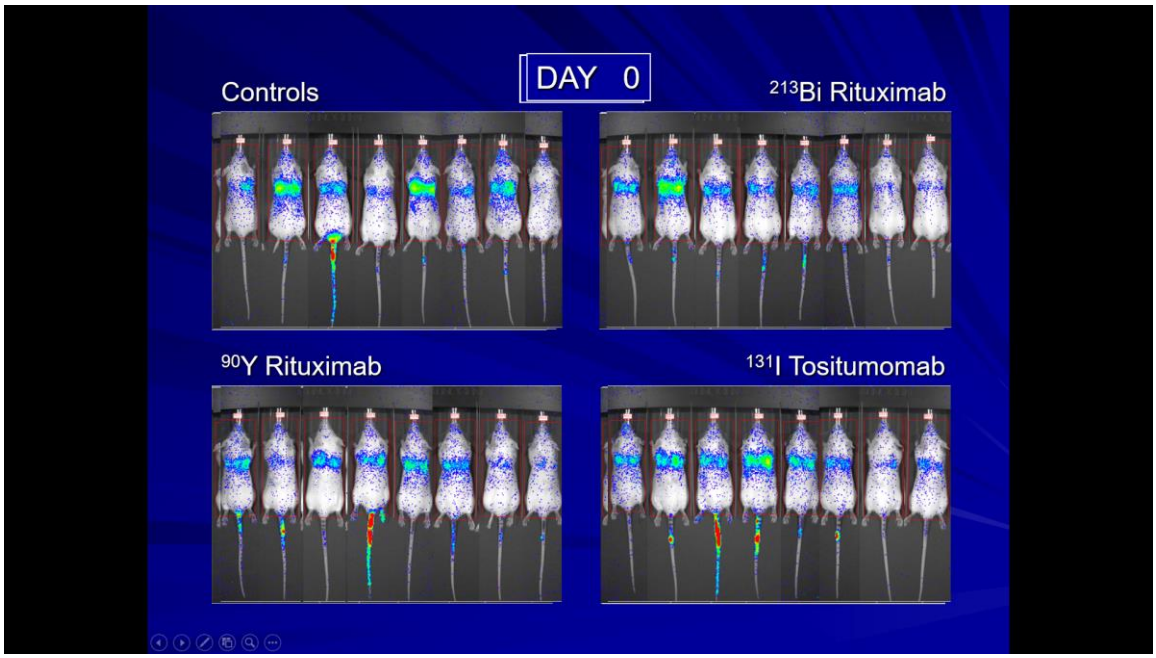

a

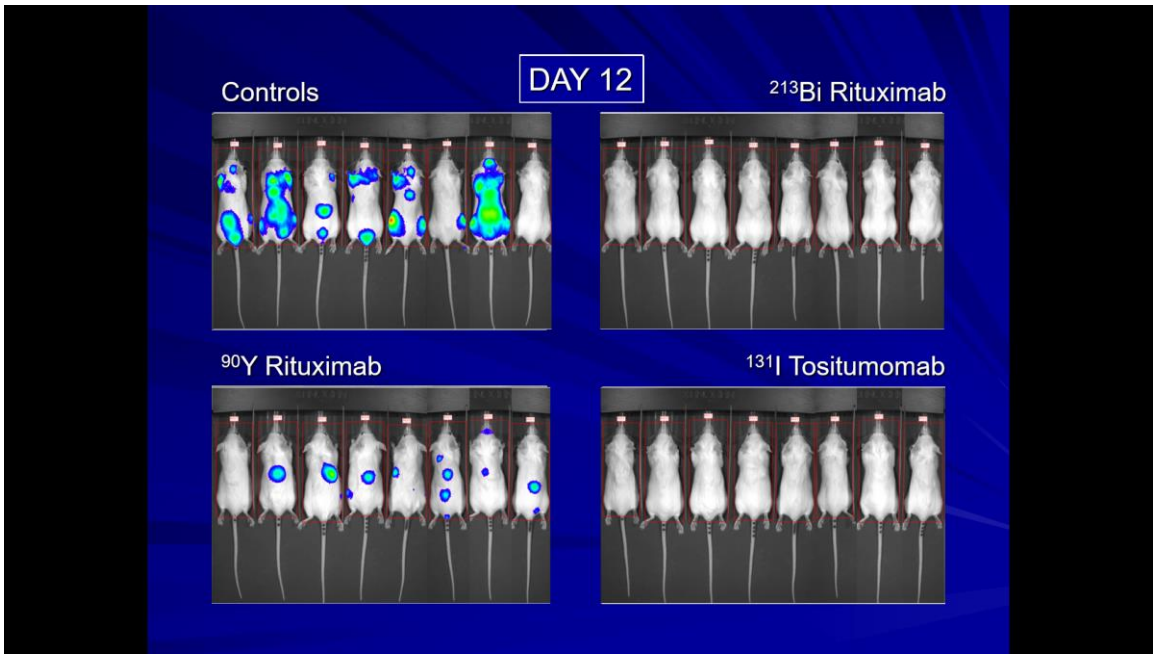

b

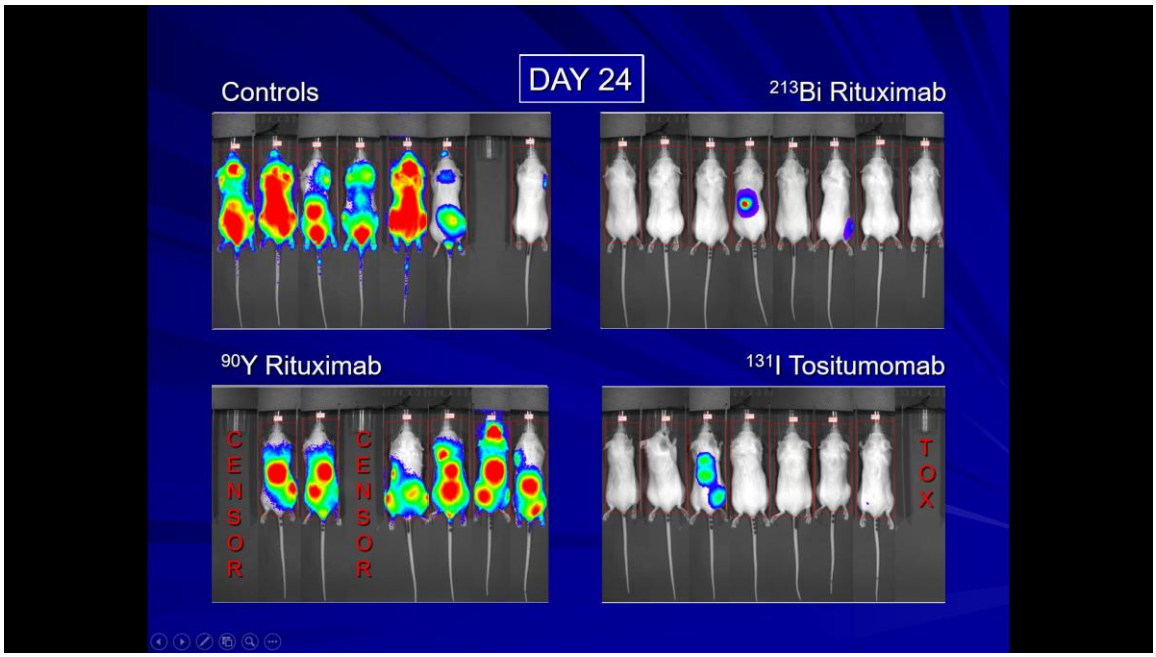

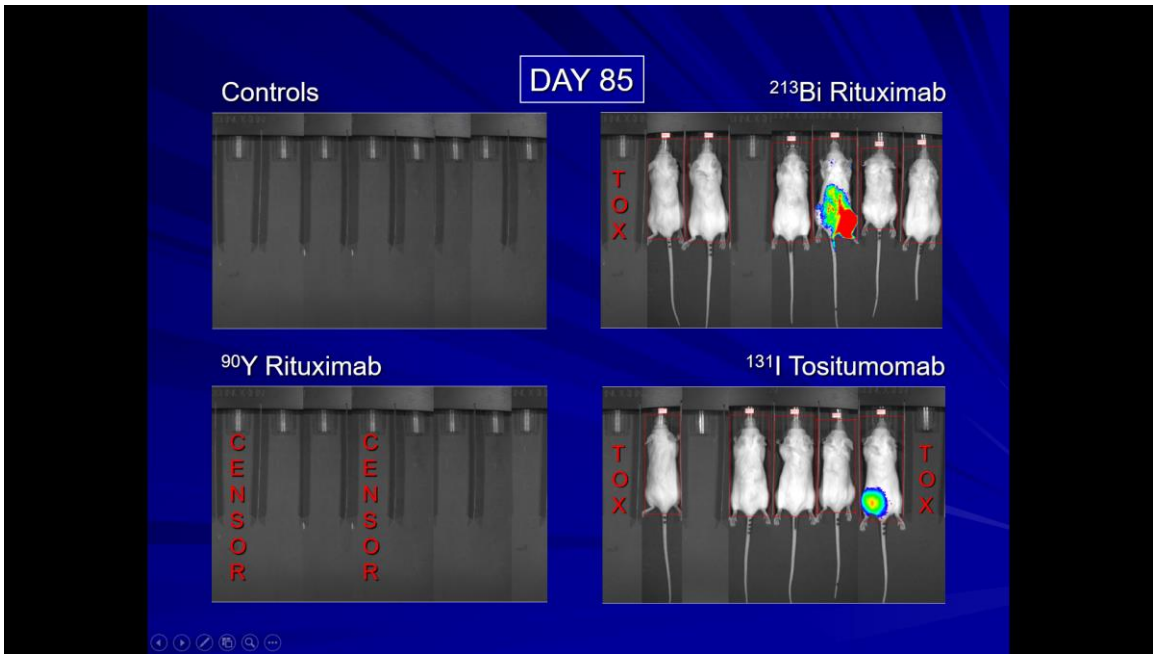

Figures 5A-D. Selected Bioluminescence Images at varying times post Rx, Experiment 4.

A single treatment was given at 4 days after injection of 10^6 tumor cells i.v.. (8 animals/group). BLI and survival were assessed. Treatment groups included controls (no rx), 10 ug unlabeled rituximab, 100 uCi ^{213}Bi rituximab, 55 uCi ^{131}I tositumomab, and 35 uCi Y-90 rituximab. Note the prolonged survival in the ^{213}Bi and ^{131}I anti CD20 groups vs controls and ^{90}Y rituximab.

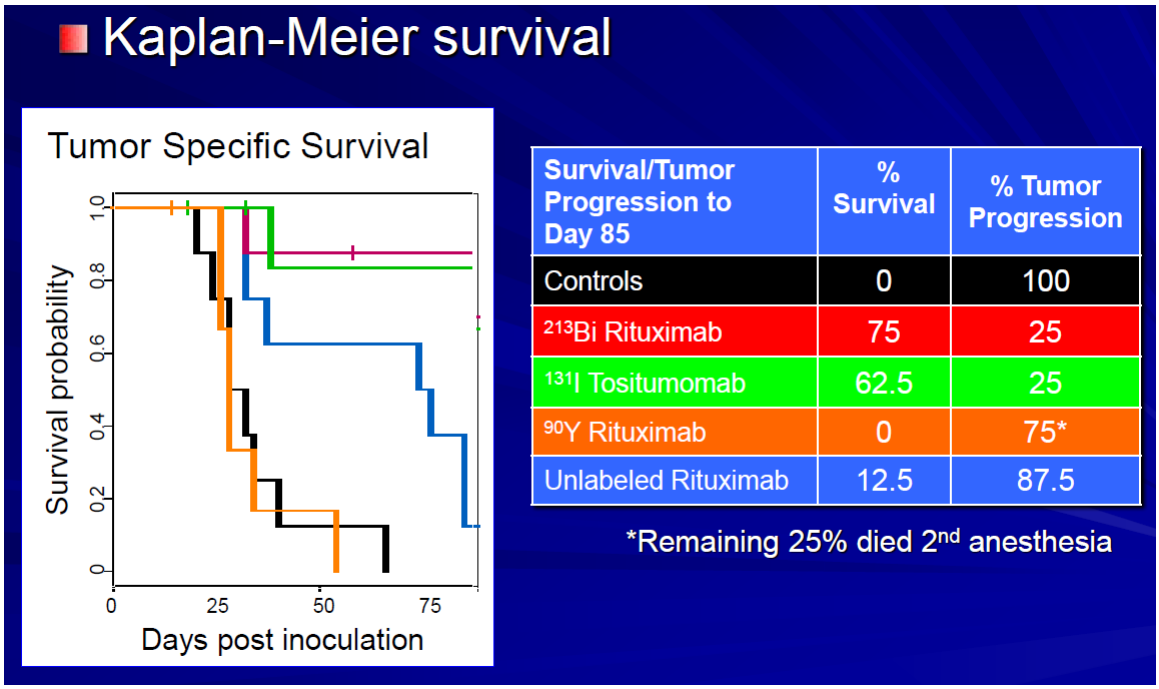

Figure 6: Experiment 4: A single treatment at 4 days post-injection of 10^6 tumor cells i.v.. 8 animals/group were studied and survival assessed. Groups included controls (no rx), 10 ug unlabeled rituximab, 100 uCi ^{213}Bi rituximab, 55 uCi ^{131}I tositumomab, and 35 uCi ^{90}Y rituximab. Cures were common with ^{213}Bi rituximab and ^{131}I tositumomab.

DETAILED MATERIALS AND METHODS:

Cells and cell culture: Epstein-Barr virus positive human Raji lymphoma tumor cells were purchased from the ATCC. The cells were lentivirally transfected with a cassette containing constitutively expressed reporter genes GFP and luciferase by Drs. Zhaohui Ye and Linzhao Cheng at The Johns Hopkins University. Stable transfection was verified via FACS quantitation of the percent of cells expressing the GFP marker (Becton-Dickinson Immunocytometry Systems, San Jose, CA) (19). Raji-GFP-Luc cells were maintained in RPMI 1600 media containing 10% fetal bovine serum (Hyclone, Utah, USA), 1% L-glutamine, 1% penicillin/streptomycin (Invitrogen Corporation, Carlsbad, CA) at 37^{o}C and 5% CO_2 in an Incubator to achieve logarithmic growth rates.

Monoclonal antibodies and antigen interaction: Rituximab (human/mouse chimeric IgG monoclonal anti-CD20) was obtained from Genentech/Biogen Idec (San Francisco, CA) and murine anti-HER-2/*neu* antibody 7.16.4 was obtained from the Sgouros laboratory (now commercially available from VWR (Radnor, PA 19087-8660) . Antibody integrity was verified via SDS-PAGE (Invitrogen Corporation, Carlsbad, CA).] Raji cell surface expression of CD20 and antibody immunoreactivity were verified by a quantitative CD20 assay followed by a competitive inhibition assay (antibody source: Quantibrite CD20 PE, BD Biosciences, San Jose, CA) performed on a FACS-Caliber quantitative flow cytometer. Similar assays were employed to confirm the absence of the her2/neu antigen on the Raji lymphoma cells. Clinical grade ^{131}I-Tositumomab was obtained from the Nuclear Medicine Pharmacy at the Johns Hopkins Outpatient Center (GSK, Philadelphia, PA).

Antibody conjugate synthesis and immunoreactivity: Monoclonal antibodies Rituximab and anti-HER-2/*neu* antibody 7.16.4 were conjugated to N-[2-amino-3-(p-isothiocyanatophenyl)propyl]-*trans*-cyclohexane-1,2-diamine-N,N',N',N'',N''-pentaacetic acid (SCN-CHX-A"-DTPA) as previously described (20) (21). Under metal-free conditions the antibodies were purified and re-suspended in conjugation buffer (50mM $NaHCO_{3-}$ Na_2CO_3, 150mM NaCl at pH 8.5) using Centricon YM-10 tubes (Millipore Corp., Bedford, MA). Re-suspended antibody was further treated with 0.5mM EDTA to scavenge any remaining free metal. The conjugation reaction was carried out using a 20-fold molar excess of SCN-CHX-A"-

DTPA incubated with antibody overnight at 25ºC. Conjugated antibody was re-purified using Centricon tubes and resuspended in 0.15mM ammonium acetate buffer. The average number of chelates per antibody was approximately 1.6 as determined by the yttrium arsenazo spectrophotometric method (22). Final antibody concentration was determined using a NanoDrop^{TM} 2000 (ThermoFisher Scientific, Waltham, MA). Immunoreactivity of radiolabeled SCN-CHX-A"-DTPA-Rituximab was determined using the method described by Lindmo *et al (23)*. Small amounts of labeled antibody (13ng per mL of cell culture) were incubated for 4 hours at 4ºC with cell aliquots containing increasing numbers of antigen targets ($7.8x10^4$ – $2.5x10^6$ CD20+ Raji cells) approaching infinite antigen excess. Cells were then thoroughly washed with cold PBS and activity levels of cell pellets and supernatant were counted separately. Immunoreactivity was calculated by extrapolation of specific binding at infinite antigen excess on a Lineweaver-Burke (double inverse) plot.

^{225}Ac/^{213}Bi generator system, mAb radiolabeling and purification: ^{225}Ac was purchased from Oak Ridge National Laboratory (Oak Ridge, TN) or from Curative Technologies Corporation (Richland, WA). The radiometal was shipped in the solid nitrate form and dissolved in 0.2M $HN0_3$ before being loaded onto supplied generators pre-packed with Chelex AG 50WX4 cation ion-exchange resin (200-400 mesh in NO_3^- form). The alpha particle emitter ^{213}Bi was eluted from an ^{225}Ac generator system that was assembled using the procedure published by McDevitt *et al (24)*. "Rituximab or antibody 7.16.4" conjugated to the chelate were incubated with BiI_4^- /BiI_5^{2-} (at 10mCi/mg) for 8 minutes in a reaction buffer (pH 4.5) containing 3mol/L ammonium acetate (Fisher Scientific) and 150mg/mL L-ascorbic acid (Sigma) preheated to 37ºC. ^{213}Bi-labeled antibody was quenched with 10µL of 100mmol/L EDTA and purified by size exclusion Microspin G-25 column (GE Healthcare Biosciences). The reaction efficiency and purity of radioimmunoconjugates were determined with instant TLC using silica gel impregnated paper (Gelman Science, Inc.)" in 2 phases (Phase I: 10mM EDTA, Phase II: 9%NaCl + 10mM NaOH). Percent recovery after purification was used in calculations to determine the specific activity of the antibody being administered. ^{90}Y-labeled Rituximab was made and purified using an essentially identical protocol, following the substitution of ^{90}Y (Perkin Elmer, Waltham, MA) for ^{213}Bi in the incubation step.

***In vitro* assays:** Following the generation of standard curves for Raji-GFP-Luc cell bioluminescence, 5 x 10^4 cells were measured on a Monolight 3010 Luminometer (Pharmingen/Becton-Dickinson) and aliquoted into 1 ml of normal growth media (described above) in a 24-well plate. Samples were divided into four groups: untreated controls, free radionuclide, and ^{213}Bi radiolabeled anti-CD20 (either blocked or unblocked with unlabeled anti-CD20). Each group receiving radioactivity was further subdivided into doses of 20μCi/ml, 10μCi/ml, or 2μCi/ml. Antigenic blockade was accomplished with a 24-hour pre-dose of unlabeled anti-CD20 at a concentration of 50μg/ml. 24 hours following the initial cell count (where radioactivity was administered), each group was transferred to 10mL of normal media in a T-25 flask. Serial counts were obtained daily for seven days or until no viable cells remained in culture. All experiments were performed in quadruplicate.

Micrometastatic B-cell lymphoma mouse model: In all experiments with tumor inoculations CB57 (CB17) Balb/c scid mice (female) purchased from Charles River Laboratories, Inc (Wilmington, MA) were intravenously injected with either 5.0 x 10^5 or 1.0 x 10^6 Raji-GFP-Luc lymphoma cells (in the exponential growth phase) suspended in 200uL phosphate buffered saline (PBS) on day 0. Immediate *in vivo* bioluminescent imaging (BLI) confirmed successful intravenous tumor injection by the presence of quantifiable signal within the lungs of each animal. In the event that no signal above pre-injection baseline was measured, d-luciferin was re-administered and the mice were imaged to confirm the absence of disseminated tumor**.** In the confirmed absence of tumor, mice were once again inoculated with intravenous tumor and re-imaged to confirm tumor dissemination.

Therapy administration: Multiple *in vivo* experiments were conducted. In each of the experiments mice previously inoculated with tumor cells were treated with experimental radiopharmaceutical ^{213}Bi -labeled Rituximab and a variety of controls. Single and multiple dose regimens were explored and compared to various controls including no treatment, free ^{213}Bi radiometal, mass equivalent doses of unlabeled Rituximab, and radiopharmaceutical ^{213}Bi-labeled anti-her2/neu (non-specific antibody). Alpha-emitter ^{213}Bi-labeled Rituximab was also compared to anti CD-20 antibodies radiolabeled with beta-emitters ^{131}I-Tositumomab and ^{90}Y-labeled Rituximab. In all except one of the experiments treatments were initiated once

exponential growth in tumor signal was established. This has been shown in our previous studies(19) to have taken place by day 7 post tumor inoculation, therefore this day was generally chosen to initiate the various therapies. Treatment was initiated at an earlier time point (day 4) in a study comparing alpha-emitter ^{213}Bi -labeled Rituximab to beta-emitters ^{131}I-Tositumomab and ^{90}Y-labeled Rituximab. The four *in vivo* experiments including tumor inoculum size, timing of treatment, dosage and frequency of radioimmunotherapy administration and various controls are summarized in **Table 1.** All radioactivity measurements were made in a Capintec dose calibrator (Capintec, Florham Park, NJ) set to 775 x 10 for ^{213}Bi, a pre-set for ^{131}I and approximately 51 x 10 for ^{90}Y immediately prior to dosing (25).

Optical imaging system and *in vivo* tracking of tumor progression: Tumor burden was followed using the Xenogen IVIS® 200 Series Imaging System (Xenogen Corp, Hopkinton, MA). Mice were injected intraperitoneally with 0.1mL of 30g/L d-luciferin (MIP, Ann Arbor, MI) 17 minutes prior to isoflurane gas anesthesia and optical imaging. Longitudinal assessment of tumor growth was done with optical imaging every 2-7 days. Each animal served as its own reference, with results normalized to baseline pre-treatment tumor burdens obtained on day 4 or day 6 depending on the experiment (12). As tumor burden increased, the necessary acquisition time decreased to an absolute minimum of 0.5s. Optical images were analyzed via software provided by the manufacturer (Xenogen Living Image 3D Analysis Package, version 1.0; Xenogen Corporation, Alameda, CA). Rectangular regions of interest were drawn around individual mice and average radiance [photons/(s)(cm^2)(sr)] was calculated by the software. This is also referred to as the relative light units per minute (RLU/min)) Mice were followed with intermittent optical imaging for 28, 131, 49, and 85 days respectively in *in vivo* experiments 1-4. In accordance with ethical guidelines, monitoring of a specific animal was discontinued in the event of a mouse death or any evidence of hind-leg paralysis (HLP) warranting euthanasia. In the first of four *in vivo* experiments animals were imaged for a preset period of four weeks, at which time all surviving animals in the study were sacrificed for pathologic analysis. In the remaining three studies intermittent imaging was continued until either all mice in a given study were experiment) or until all mice in the study with any evidence of tumor progression were deceased (experiments 2 and 4). In the latter category, mice without evidence of tumor progression were imaged for an additional several weeks following the final tumor-related death

in the study to ensure they did not develop bioluminescent signal in excess of baseline as evidence of tumor progression. In all except experiment 1, overall survival was assessed by monitoring the mice, after the imaging period had ended, until death or hind limb paralysis developed or when sacrifice of remaining animals was required for logistical reasons.

Statistical analysis: **General Statistical Strategy:**

In each study, two major parameters were typically assessed: The time from treatment until death (or hind limb paralysis necessitating sacrifice), assessed by Kaplan Meier analysis, analysis of variance and t-tests. In addition, the RLU was monitored, which was also followed for each animal before and at multiple time points after therapy. A log transformation was applied to normalized RLU to analyze data from day 6 onward. For normalized RLU before day 6, no transformation is used. A mixed effects model with exchangeable correlation structure for longitudinal repeated measures was fitted for each group separately to estimate its normalized RLU growth rate after day 6 (the baseline day). Pair-wise comparisons between groups were made using random effects model with covariates group, day, and their interaction. For normalized RLU before day 6, analysis of variance is used. Calculations were performed using SAS, Carey NC.

Histologic examination: Representative animals were identified for pathological assessment at 28 days post tumor inoculation in experiment 1, when their disease had progressed sufficiently that humane sacrifice was required and when the studies were terminated with no evidence of tumor progression in experiments 2-4. For histology, CNS, bone marrow, spleen, kidney, and lung tissues were fixed in 10% buffered formalin, processed and embedded in paraffin, and sectioned at 5μm. Sections were stained with hematoxylin and eosin and examined via light microscopy by a senior faculty member of the animal pathology department (RH). Blood smears were made from peripheral blood samples and stained with a modified giemsa stain. These assessments were qualitative and descriptive.

Supplemental Results:

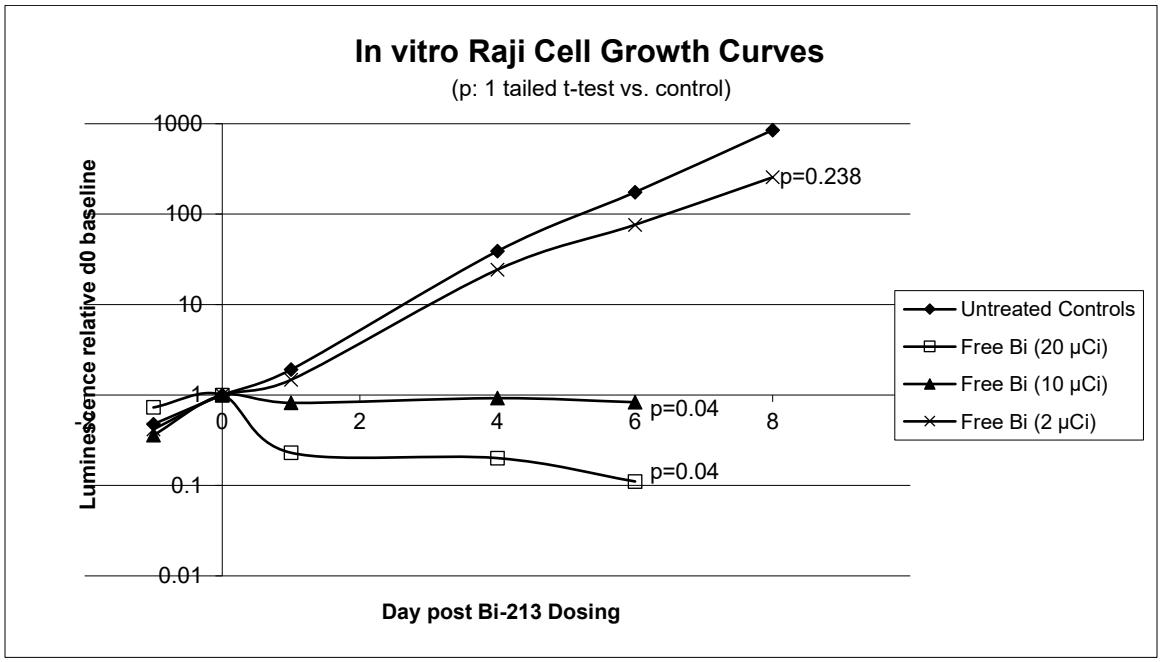

Supplemental figure 1: In vitro Raji lymphoma cell growth curves, with or without free radionuclide administration. Results are displayed on a logarithmic scale. There is dose dependent cell kill with free ^{213}Bi. P values assess differences between controls and the varying treatment quantities of free ^{213}Bi.

	^{213}Bi *Ritux. (100 uCi) ATB=8*	^{213}Bi *Ritux (35 uCi) ATB=40*	*Unlabeled Rituximab ATB=397*	*Free* ^{213}Bi *(35 uCi) ATB=265*	^{213}Bi *Herceptin ATB =143*
No Tx ATB=1545	***.0309***	***.0183***	*.0916*	*.0635*	***.0295***
^{213}Bi *Herceptin*	***.0237***	***.0236***	*.1866*	*.0744*	
Free ^{213}Bi	***.0232***	***.0152***	*.239*		
Unlabeled Rituximab	***.0244***	*.0182*			
^{213}Bi *Rituximab (35 uCi)*	*.1016*				

Supplemental Table 1: Study 1 compares average day 18 tumor burdens (ATB) from BLI among study groups. Relative increase in tumor burden (normalized to day four) is indicated in headers, significant results are bolded. ATB is lowest with the 100 uCi dose of ^{213}Bi *Rituximab and highest in the control group. A* ^{213}Bi *Rituximab dose response relationship is apparent.*

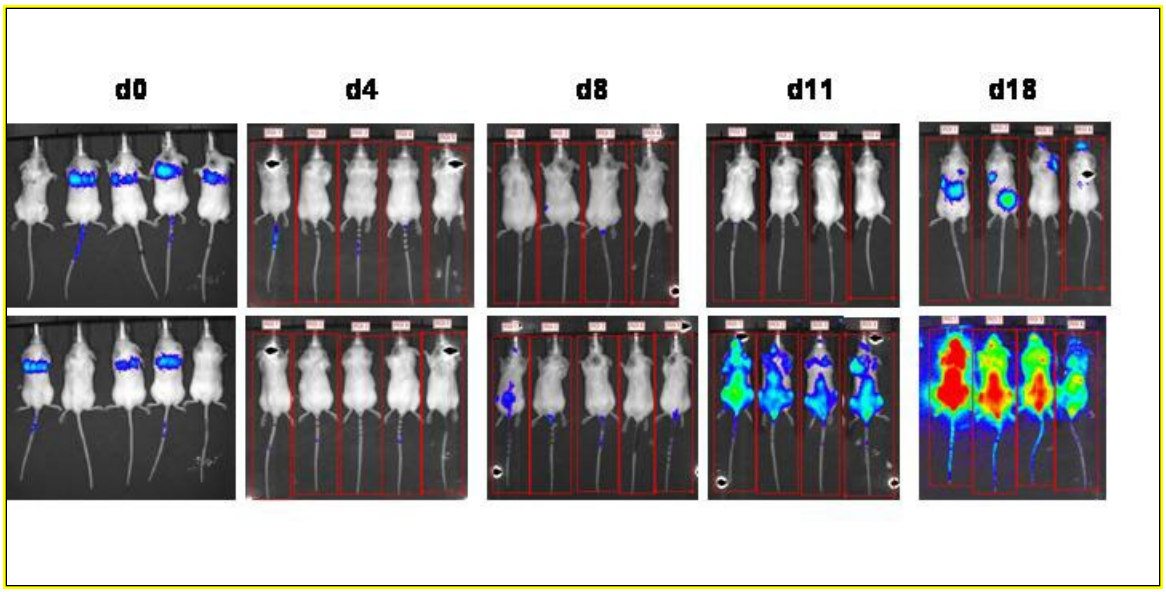

Supplemental Figure 2: Representative data sets of sequential optical image acquisitions in Experiment 1. Top row: mice treated with 100μCi dose of ^{213}Bi-labeled rituximab. Bottom row: untreated controls. The window parameters the same for all pictures for ease of comparison (minimum: 4.0×10^4; maximum: 1.0×10^7 photons/m^2/s). On day 0, note the localization of tumor signal to the lungs in mice successfully dosed with tumor. By day 4, reliable quantitation of tumor signal is possible (but not easily visible on the windowing scale employed here). On day 18, tumor signal is finally seen in the treatment group but is qualitatively and quantitatively less than that in the control group.

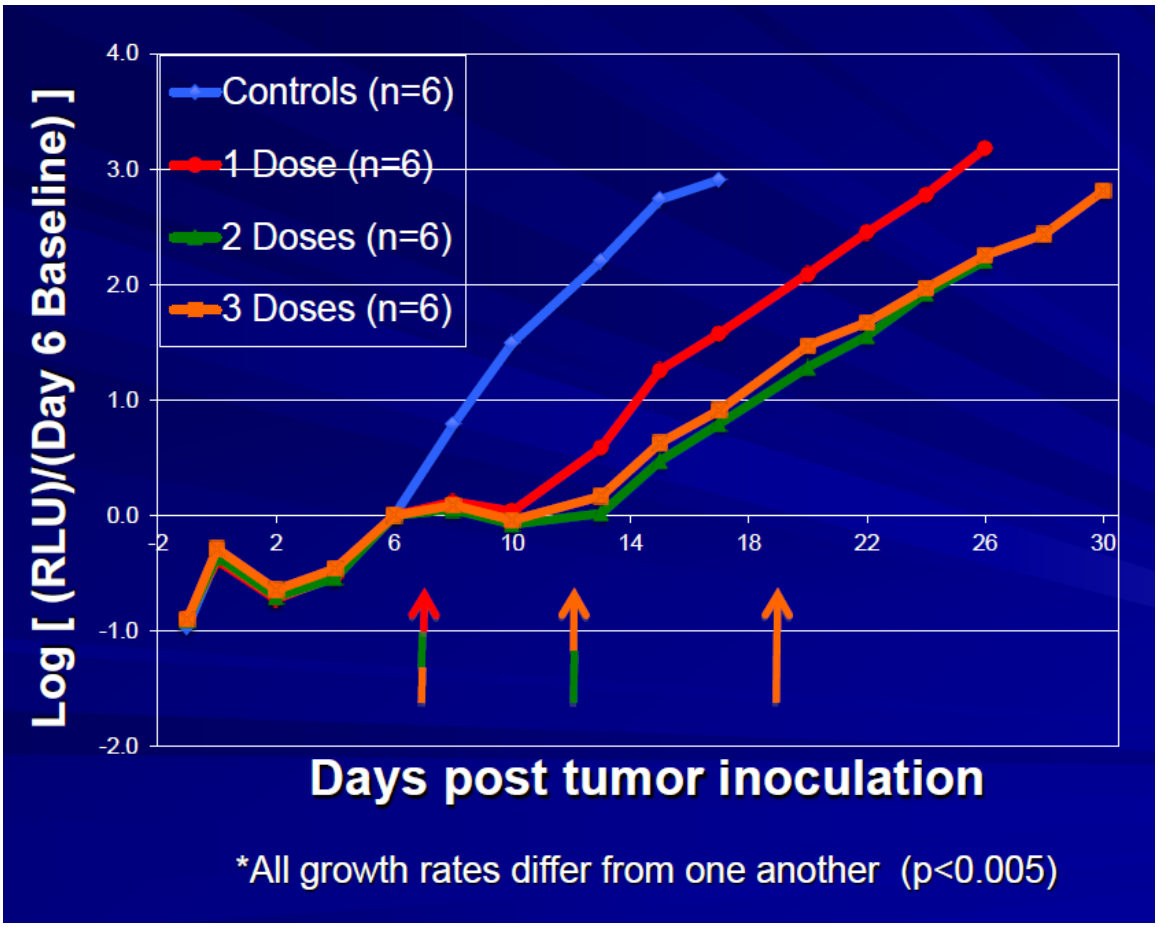

Supplemental figure 3: Experiment 3
In this experiment we evaluated repeated dosing to see if it could delay progression of slightly more advanced disease. Twice the tumor burden of initial experiments (1 million cells) was injected on Day 0. All groups but the control group were treated with 75uCi ^{213}Bi Rituximab with 1,2, or 3 doses on Days 7,12,19. Notable findings include: following initial treatment on Day 7 there is a BLI tumor regression and a clear delay tumor progression relative to controls in blue. A further delay in tumor growth is seen with repeat dosing on day 12 relative to single dosing, green and orange versus red, while there is still relatively low tumor burden. No clear additional benefit was seen with a 3rd dose on day 19 once tumor has progressed to approximately 10-fold the pretreatment baseline.

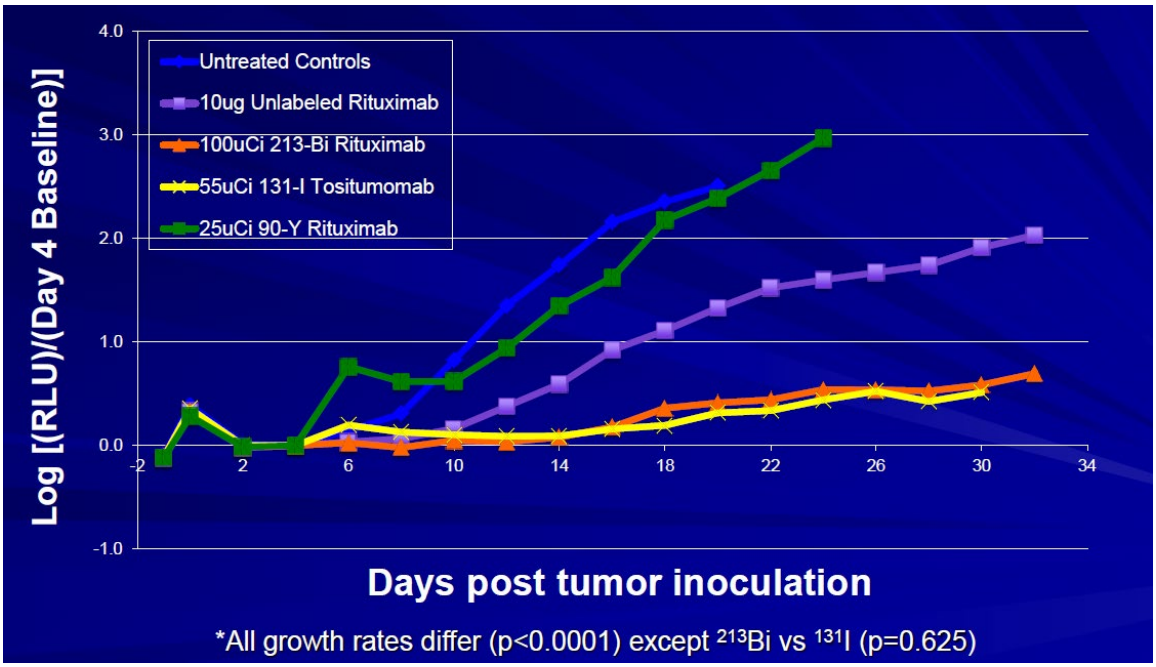

Supplemental Figure 4. Experiment 4: Mean Log of RLU/baseline (day 4) in varying treatment groups receiving a single treatment dose. Note the prolonged tumor growth delays in the ^{213}Bi rituximab and ^{131}I tositumomab groups.

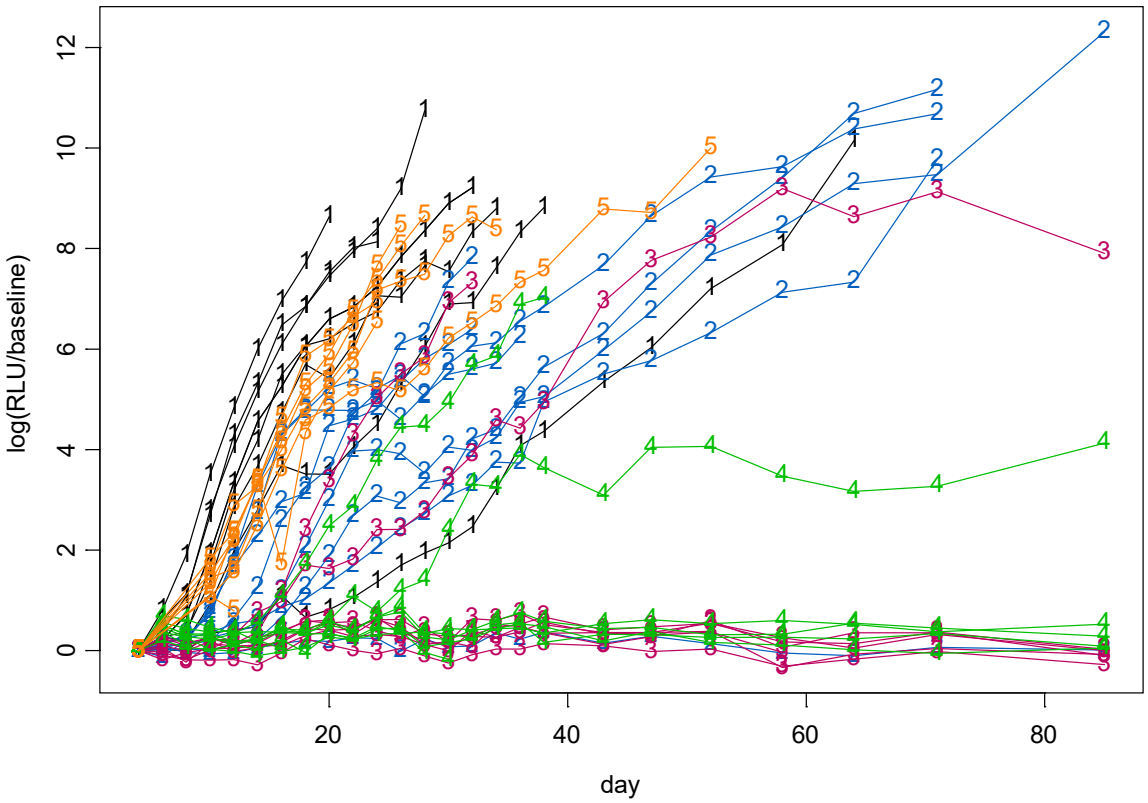

Supplemental Figure 5: Individual animal BLI data from experiment 4.

Group

1 Controls
2 Mass Equivalent Dose Cold Rituximab
3 One Dose ^{213}Bi i Rituximab (100uCi)
4 One Dose ^{131}I Tositumomab (55uCi)
5 One Dose ^{90}Y Rituximab (25uCi)

Supplemental Data:

Detailed Statistical Output from a representative study (study 4):

Supplemental Data Study 4:

Group	
1	Controls
2	Mass Equivalent Dose Cold Rituximab
3	One Dose 213Bi Rituximab (100uCi)
4	One Dose 131-I Tositumomab (55uCi)
5	One Dose 90-Y Rituximab (25uCi)

Box plot of normalized RLU from day 4

Supplemental figure 6.

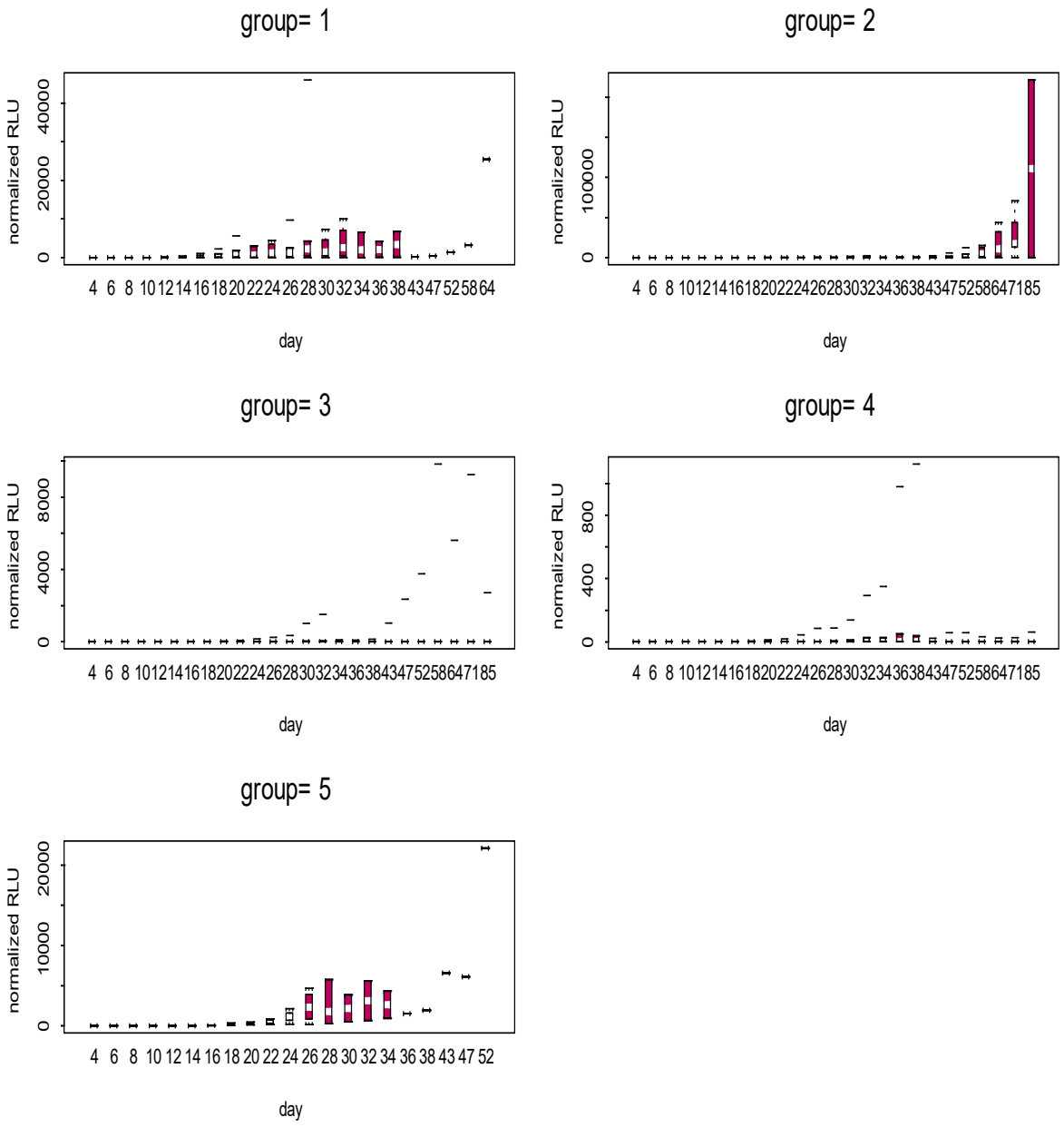

Supplemental figure 6.

Supplemental figure 7:

Since data are highly skewed, log transformation is applied to the data. Box plot of log transformed normalized RLU:

Group

1 Controls
2 Mass Equivalent Dose Cold Rituximab
3 One Dose 213Bi Rituximab (100uCi)
4 One Dose 131-I Tositumomab (55uCi)
5 One Dose 90-Y Rituximab (25uCi)

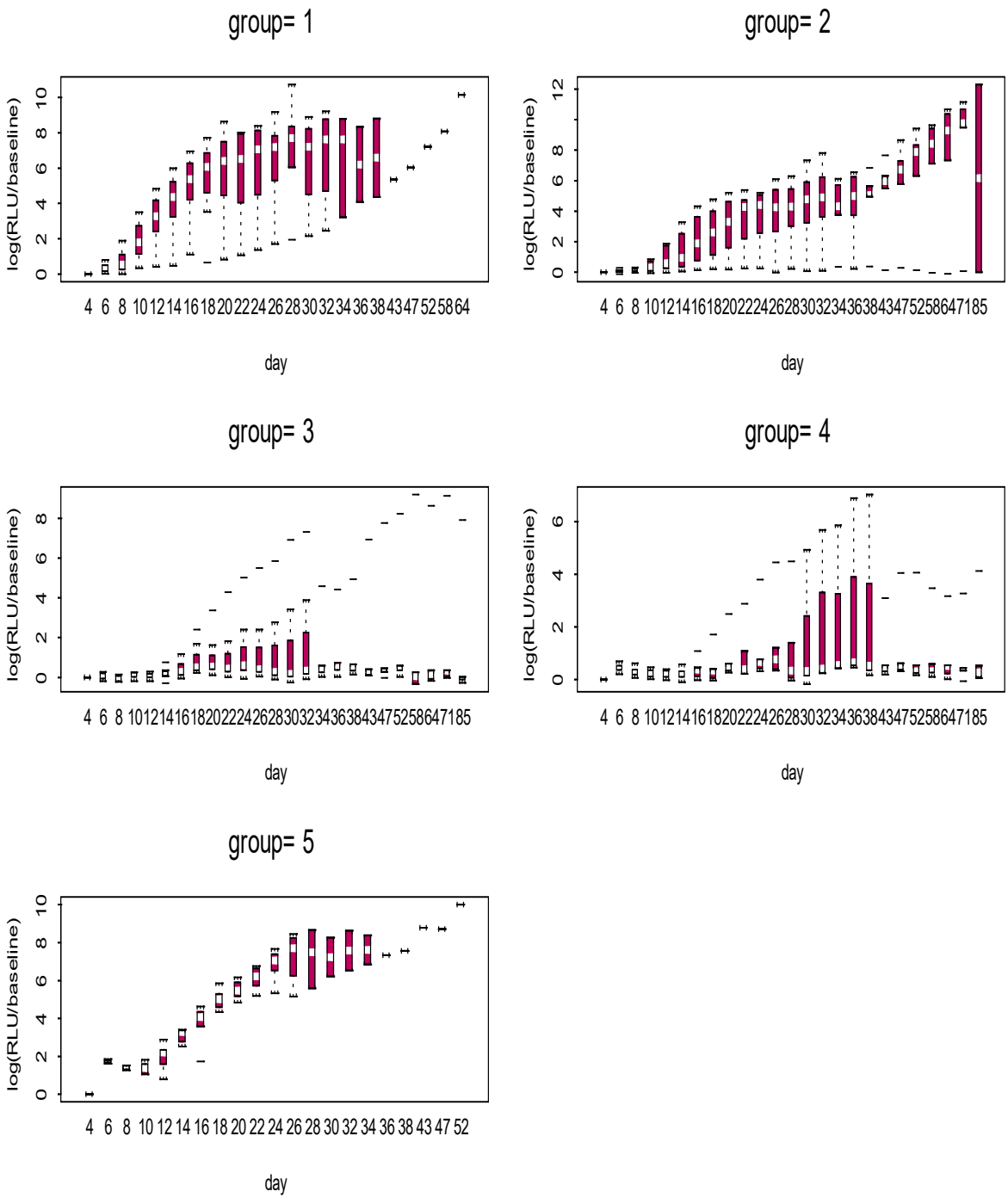

Supplemental figure 7.

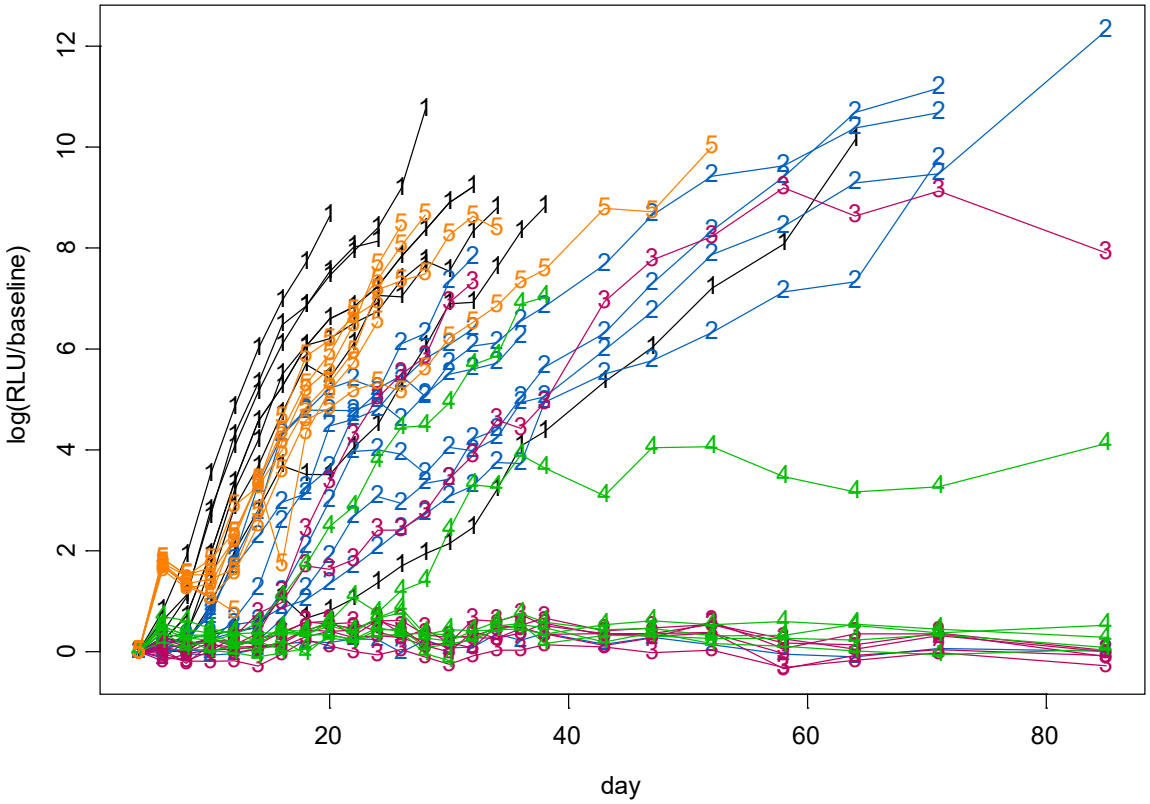

Group

1 Controls
2 Mass Equivalent Dose Cold Rituximab
3 One Dose 213Bi Rituximab (100uCi)
4 One Dose 131-I Tositumomab (55uCi)
5 One Dose 90-Y Rituximab (25uCi)

Supplemental figure 8a .

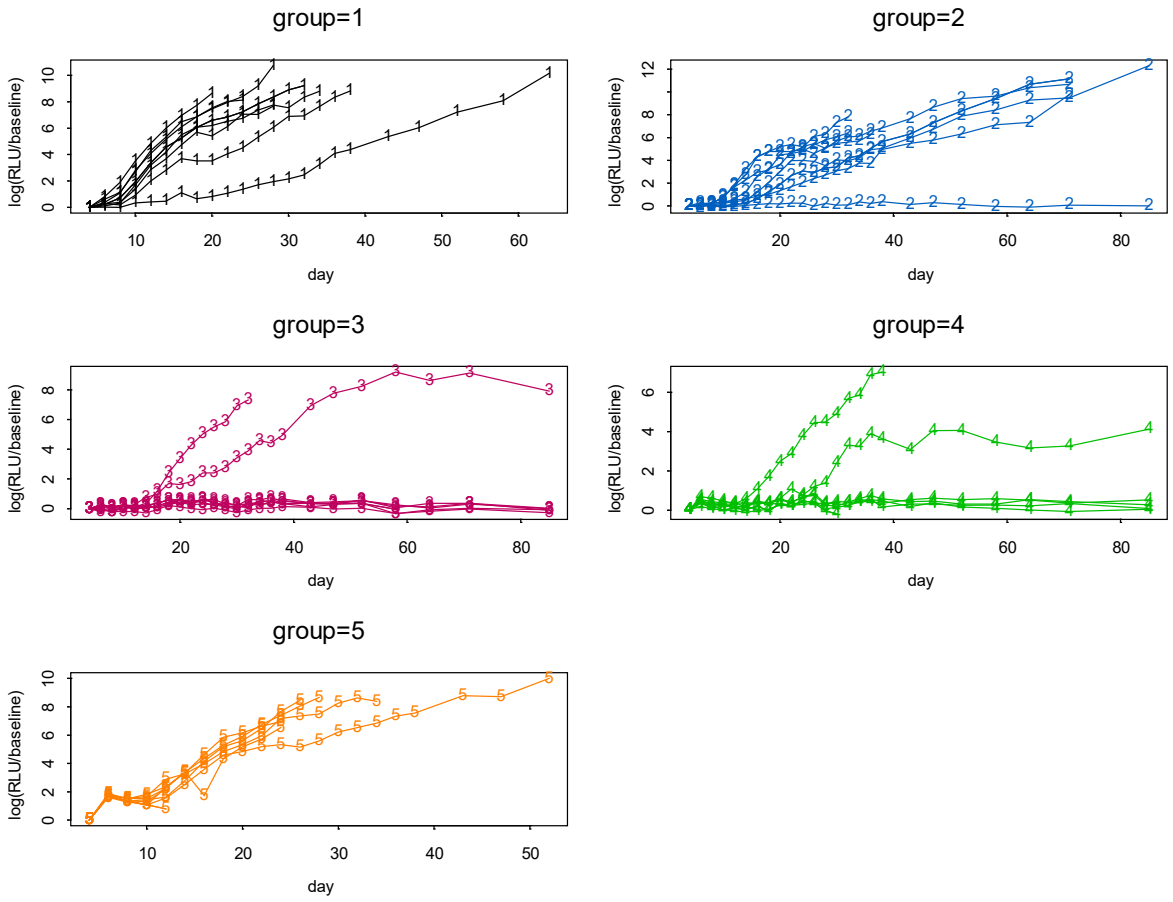

Supplemental figure 8b.

Results

A1. Increase rate of log(RLU/baseline) in time from day 6, i.e., the slope of (Day – 6), in different groups.

Group	# animals	# observation	value	Standard error	P value
1	8	118	0.1871	0.0176	<.0001
2	8	169	0.1221	0.0088	<.0001
3	8	187	0.0249	0.0058	<.0001
4	8	164	0.0165	0.0051	0.0016
5	8	94	0.2490	0.0103	<.0001

Conclusion: the RLU in all 5 groups increase over time (all $p<0.01$). The reason that group 1 has lower slope value is because one animal has much lower RLU than all other animals in group 1 and all animals in group 5.

Supplemental table 2.

A2. Pair-wise group comparison

A2.1 From day 4 (baseline) (Supplemental table 3)

We applied linear mixed effects model with exchangeable correlation structure among repeated measures for response variable log(RLU/baseline).

Reference group	Treatment group	Group by day interaction	Standard error	P value
1	2	-0.0995	0.0127	<.0001
1	3	-0.2044	0.0114	<.0001
1	4	-0.2053	0.0101	<.0001
1	5	0.0288	0.0143	0.0459
2	3	-0.1033	0.0071	<.0001
3	4	-0.0027	0.0055	0.6251
3	5	0.2429	0.0115	<.0001
4	5	0.2428	0.0088	<.0001

Conclusion: The increase of normalized RLU in each of the groups 2-5 is much slower than group 1 ($p<0.05$ for all 4 comparisons). The RLU in group 5 increases much faster than groups 3 and 4 ($p<0.0001$). There is no significant difference between group 3 and group 4 ($p=0.6251$).

Group

1 Controls
2 Mass Equivalent Dose Cold Rituximab
3 One Dose 213Bi Rituximab (100uCi)
4 One Dose 131-I Tositumomab (55uCi)
5 One Dose 90-Y Rituximab (25uCi)

A2.2 Before baseline day (i.e., all observations from before day 4)
The analysis of variance of normalized RLU is used. No significant difference in all pairwise group comparisons (all p>0.18).

A2.3 Compare survival outcome
Death
0 Alive
1 Hind limb Paralysis (HLP)
2 Found dead (Tumor-related: Significant bioluminescence signal on recent imaging)
3 Found dead (Non Tumor-related: No/minimal bioluminecence signal on recent imaging)
4 Found dead (Unknown: No recent imaging prior to time of death)*
5 Accidental premature death (No recent tumor signal)
6 Accidental premature death (Recent increasing tumor signal)
7 Hind limb Paralysis (HLP): No/minimal bioluminescence signal on recent imaging

Event1 =1(if the death code is1, or 2), 0(otherwise).
Event2 =1(if the death code is1, 2, or 3), 0(otherwise).

In the dataset, event1 is identical to event2.

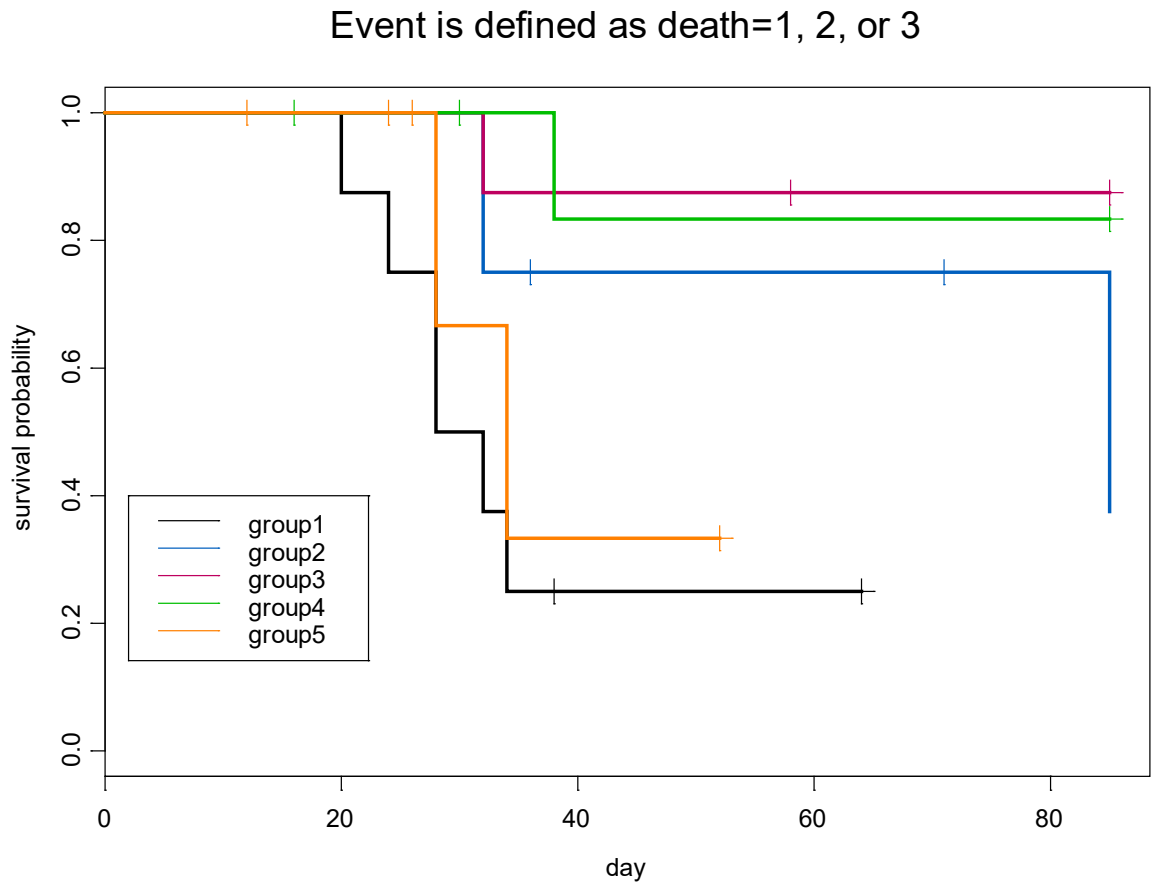

Supplemental figure 9

Cox proportional hazards model: **(Supplemental table 4)**

Reference group	Treatment group	Treatment group HR	Standard error (HR)	P value
1	2	-2.22	0.821	0.0069
1	3	-1.57	0.543	0.0038
1	4	-0.998	0.363	0.0060
1	5	-0.136	0.204	0.5000
2	3	-1.61	1.17	0.17
3	4	0.248	1.41	0.86
3	5	1.39	0.614	0.024
4	5	2.71	1.23	0.028

A2.4 Compare survival time to minimal significant disease progression which is defined as the first significant amount change in log(RLU/baseline) observed from the control group

The median log(RLU/baseline) in control group (group=1) increases significantly at day 6 (median 0.2724, p=0.0078, signed rank test) and continues to increase at later days. We thus use 0.28 as the threshold of log(RLU/baseline) to define minimal significant disease progression and the corresponding onset time. We then compare Kaplan-Meier survival curves of this event onset time between groups.

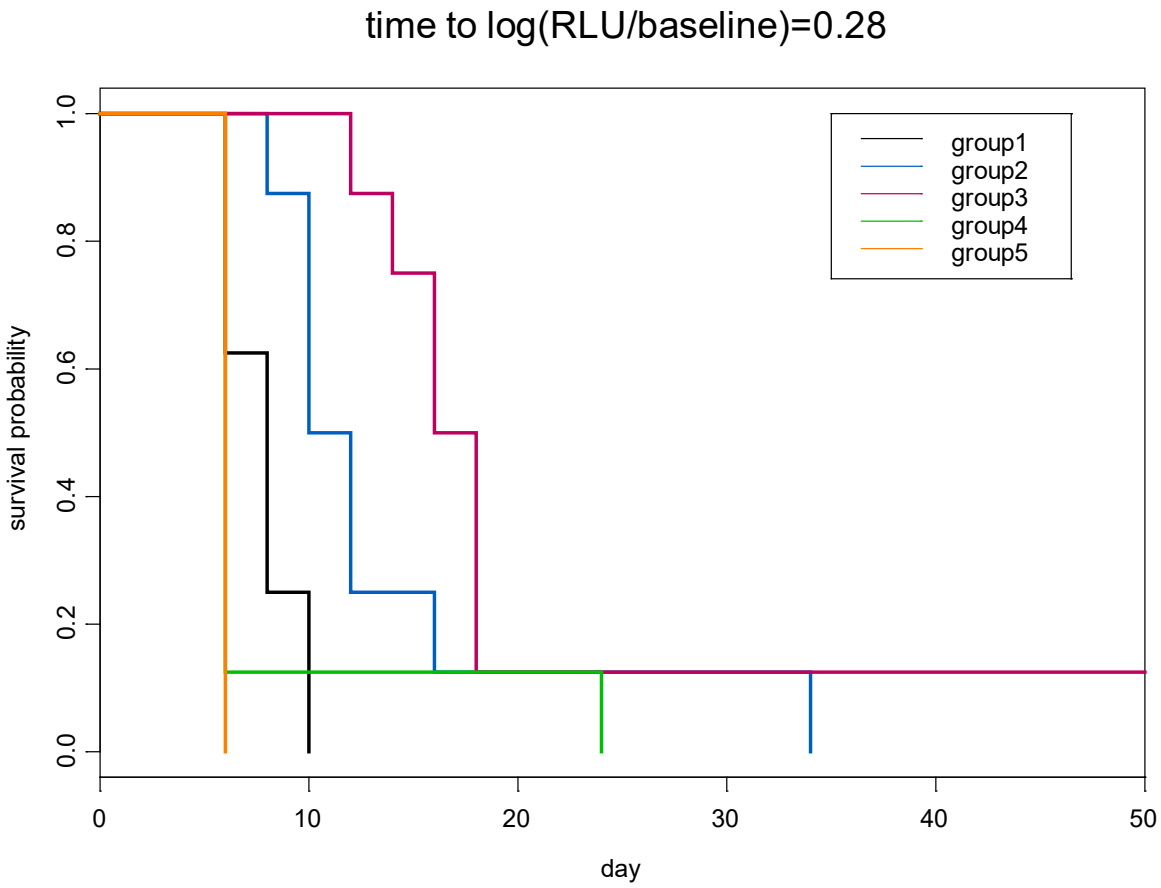

Supplemental Figure 10. Note: If a short symptomatic effect is present, then the above comparisons are only suitable for symptomatic effect.

	n.obs	n.max	n.first	events	mean	se(mean)	median	0.95LCL	0.95UCL
group=1	8	8	8	8	7.75	0.552	8	6	NA
group=2	8	8	8	8	14.00	2.784	11	8	16
group=3	8	8	8	7	24.63	8.099	17	12	18
group=4	8	8	8	8	8.25	2.105	6	6	6
group=5	8	8	8	8	6.00	0.000	6	NA	NA

A2.5 Compare survival time to 30-day control group median disease progression in log(RLU/baseline)

Supplemental table 5.

The control group 31-day median log(RLU/baseline) value is 7.22

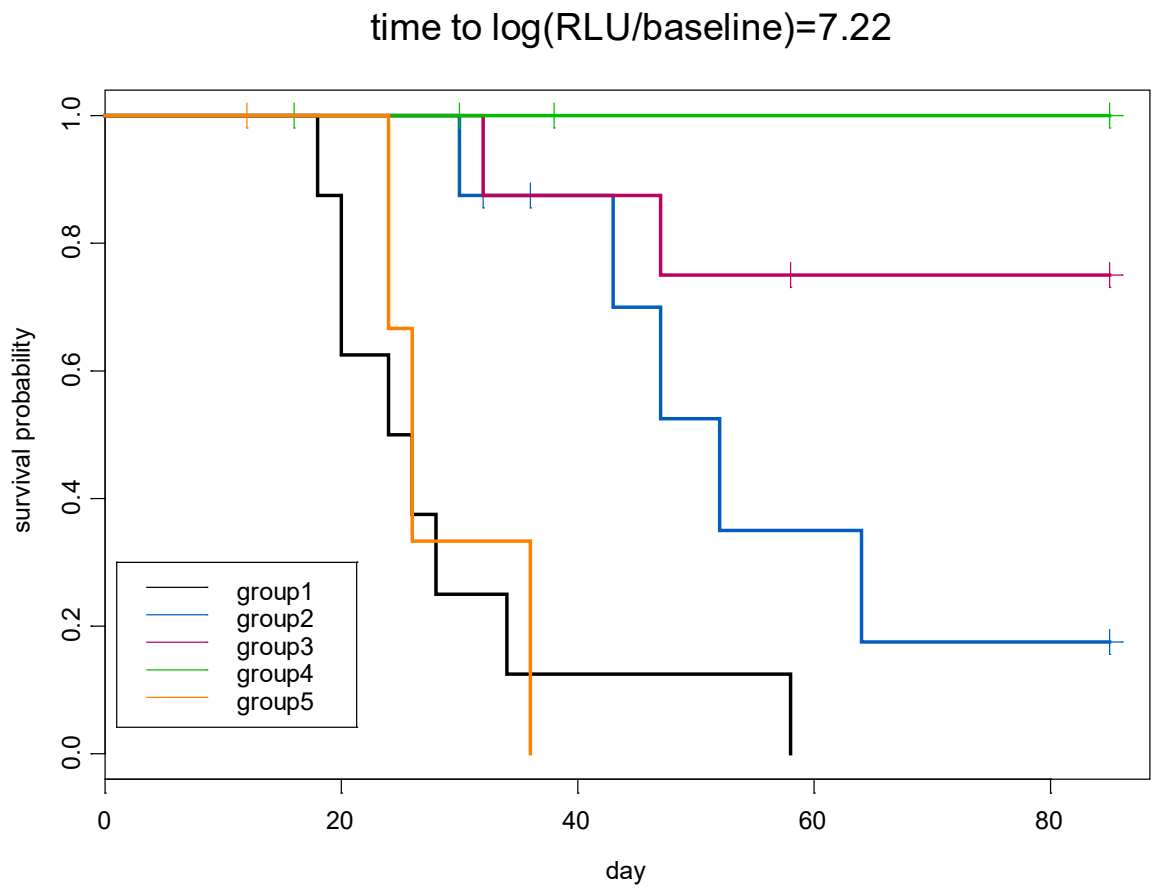

Supplemental figure 11.

	n.obs	n.max	n.first	events	mean	se(mean)	median	0.95LCL	0.95UCL
group=1	8	8	8	8	28.5	4.30	25	18	34
group=2	8	8	8	5	54.7	6.78	52	30	NA
group=3	8	8	8	2	73.6	7.09	NA	32	NA
group=4	8	8	8	0	85.0	0.00	NA	NA	NA
group=5	8	8	8	4	28.7	2.71	26	24	NA

Supplemental table 6.

A2.6 Compare disease progression rate among non-cured animals

From spaghetti plot of all animals, we define those animals whose log(RLU/baseline) value is below 2 after day 60 as "cured" animals. These 10 animals have ID= 10 18 19 21 23 24 26 28 29 30

Remove the 10 “cured” animals and compare disease progression rate among non-cured animals:

Group	# animals	# observation	Value(slope)	Standard error	P value
1	8	118	0.1871	0.0176	<.0001
2	7	144	0.1628	0.0051	<.0001
3	3	62	0.1049	0.0096	<.0001
4	4	64	0.0831	0.0071	<.0001
5	8	94	0.2490	0.0103	<.0001

Supplemental table 7.